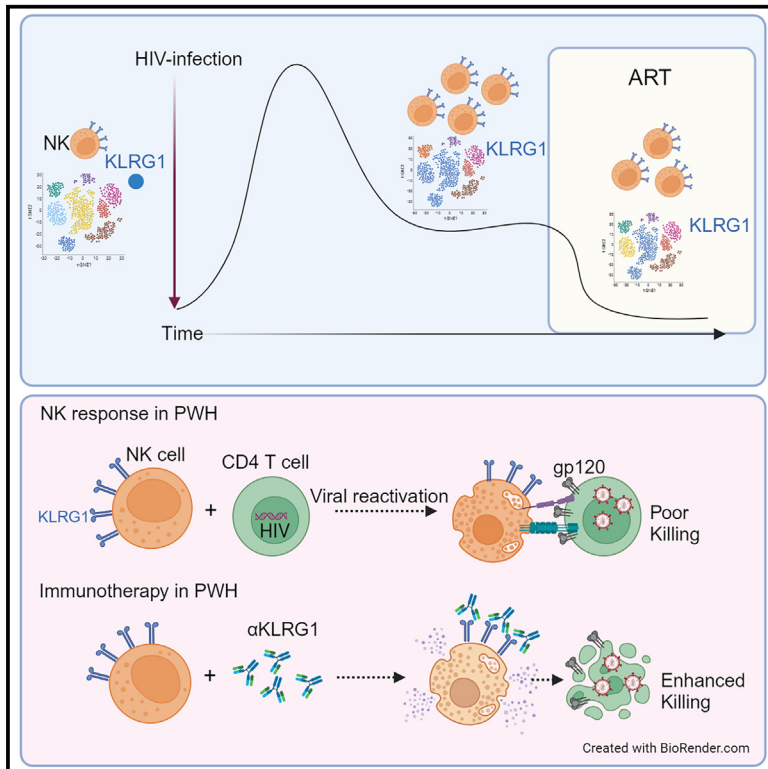


# KLRG1 expression on natural killer cells is associated with HIV persistence, and its targeting promotes the reduction of the viral reservoir

## Graphical abstract



## Authors

Antonio Astorga-Gamaza, David Perea, Nerea Sanchez-Gaona, ..., Meritxell Genescà, Enrique Martín-Gayo, Maria J. Buzon

## Correspondence

mariajose.buzon@vhir.org

## In brief

Human immunodeficiency virus (HIV) infection induces immune dysfunction. Astorga-Gamaza et al. show that targeting KLRG1—an immune checkpoint receptor—on natural killer (NK) cells from people with HIV enhances NK activity and reduces the latent HIV reservoir. The results suggest that targeting NK cells could potentially aid in the elimination of HIV-infected cells.

## Highlights

- The expression of KLRG1 on NK cells correlates with active HIV transcription
- NK cells with KLRG1 expression exhibit functional impairment
- Targeting KLRG1 enhances the capacity of NK cells
- Antibodies directed against KLRG1 promote a reduction in intact HIV genomes



## Article

# KLRG1 expression on natural killer cells is associated with HIV persistence, and its targeting promotes the reduction of the viral reservoir

Antonio Astorga-Gamaza,<sup>1,6</sup> David Perea,<sup>1,6</sup> Nerea Sanchez-Gaona,<sup>1</sup> Marta Calvet-Mirabent,<sup>2,3</sup> Ana Gallego-Cortés,<sup>1</sup> Judith Grau-Expósito,<sup>1</sup> Ildefonso Sanchez-Cerrillo,<sup>2,3</sup> Joan Rey,<sup>1</sup> Josep Castellví,<sup>4</sup> Adrian Curran,<sup>1</sup> Joaquín Burgos,<sup>1</sup> Jordi Navarro,<sup>1</sup> Paula Suanzes,<sup>1</sup> Vicenç Falcó,<sup>1</sup> Meritxell Genescà,<sup>1</sup> Enrique Martín-Gayo,<sup>2,3,5</sup> and Maria J. Buzon<sup>1,7,\*</sup>

<sup>1</sup>Infectious Diseases Department, Hospital Universitari Vall d'Hebron, Institut de Recerca (VHIR), Universitat Autònoma de Barcelona, 08035 Barcelona, Spain

<sup>2</sup>Universidad Autónoma de Madrid, 28049 Madrid, Spain

<sup>3</sup>Immunology Unit from Hospital Universitario de La Princesa and Instituto de Investigación Sanitaria Princesa, 28006 Madrid, Spain

<sup>4</sup>Department of Pathology, Hospital Vall d'Hebron, Universitat Autònoma de Barcelona, 08035 Barcelona, Spain

<sup>5</sup>Infectious Diseases CIBER (CIBERINFEC), Instituto de Salud Carlos III, 28029 Madrid, Spain

<sup>6</sup>These authors contributed equally

<sup>7</sup>Lead contact

\*Correspondence: [mariajose.buzon@vhir.org](mailto:mariajose.buzon@vhir.org)

<https://doi.org/10.1016/j.xcrm.2023.101202>

## SUMMARY

Human immunodeficiency virus (HIV) infection induces immunological dysfunction, which limits the elimination of HIV-infected cells during treated infection. Identifying and targeting dysfunctional immune cells might help accelerate the purging of the persistent viral reservoir. Here, we show that chronic HIV infection increases natural killer (NK) cell populations expressing the negative immune regulator KLRG1, both in peripheral blood and lymph nodes. Antiretroviral treatment (ART) does not reestablish these functionally impaired NK populations, and the expression of KLRG1 correlates with active HIV transcription. Targeting KLRG1 with specific antibodies significantly restores the capacity of NK cells to kill HIV-infected cells, reactivates latent HIV present in CD4<sup>+</sup> T cells co-expressing KLRG1, and reduces the intact HIV genomes in samples from ART-treated individuals. Our data support the potential use of immunotherapy against the KLRG1 receptor to impact the viral reservoir during HIV persistence.

## INTRODUCTION

Antiretroviral therapy (ART) currently available for treating the human immunodeficiency virus (HIV) infection generally controls viral replication in people with HIV (PWH), but it is not curative.<sup>1</sup> ART cannot prevent the formation nor achieve the complete elimination of a population of cells, mainly CD4<sup>+</sup> T cells, which form the viral reservoir. The HIV reservoir is located in cells from the blood and several other tissues and harbors integrated provirus, the majority containing viral sequences with deleterious defects. However, a small fraction contains replication-competent proviruses that can initiate new rounds of infection if ART is interrupted.<sup>2</sup> Several factors may facilitate HIV persistence, such as the predominant state of viral latency, cell proliferation, and mechanisms of immune evasion that might allow infected cells to survive even when cells are actively transcribing HIV.<sup>3</sup> Moreover, chronic viral infection is associated with elevated immune activation and deteriorated immune responses in PWH, including those mediated by natural killer (NK) cells.<sup>4,5</sup> Importantly, ART does not fully revert immune exhaustion,<sup>6,7</sup> and therapies directed to boost the immune responses will likely be

needed to accelerate the elimination of the persistent HIV reservoir.

NK cells are potential candidates for immunotherapy given their strong cytotoxic responses against many infectious pathogens and malignant cells. NK cells have several mechanisms of action, exerting innate responses that do not require prior exposure to antigens, but also cellular responses linked to adaptive immunity such as the antibody-dependent cellular cytotoxicity (ADCC) response, and, as it has recently been evidenced, the capacity to develop memory-like features against several viruses.<sup>8–10</sup> Understanding the functional properties of NK cells during HIV infection could help to exploit their full potential to reduce HIV reservoirs. NK cells have also become increasingly appreciated in the context of “shock and kill” approaches. This strategy is currently being pursued to target latent HIV using latency reversal agents (LRAs) to induce viral expression and potentiate the killing of infected cells through the boosting of immune cells.<sup>11</sup> In this regard, in a humanized mouse study, the combination of LRAs together with the exogenous administration of NK cells significantly diminished the *in vivo* HIV reservoir.<sup>12</sup> Moreover, in a clinical study designed to disrupt viral



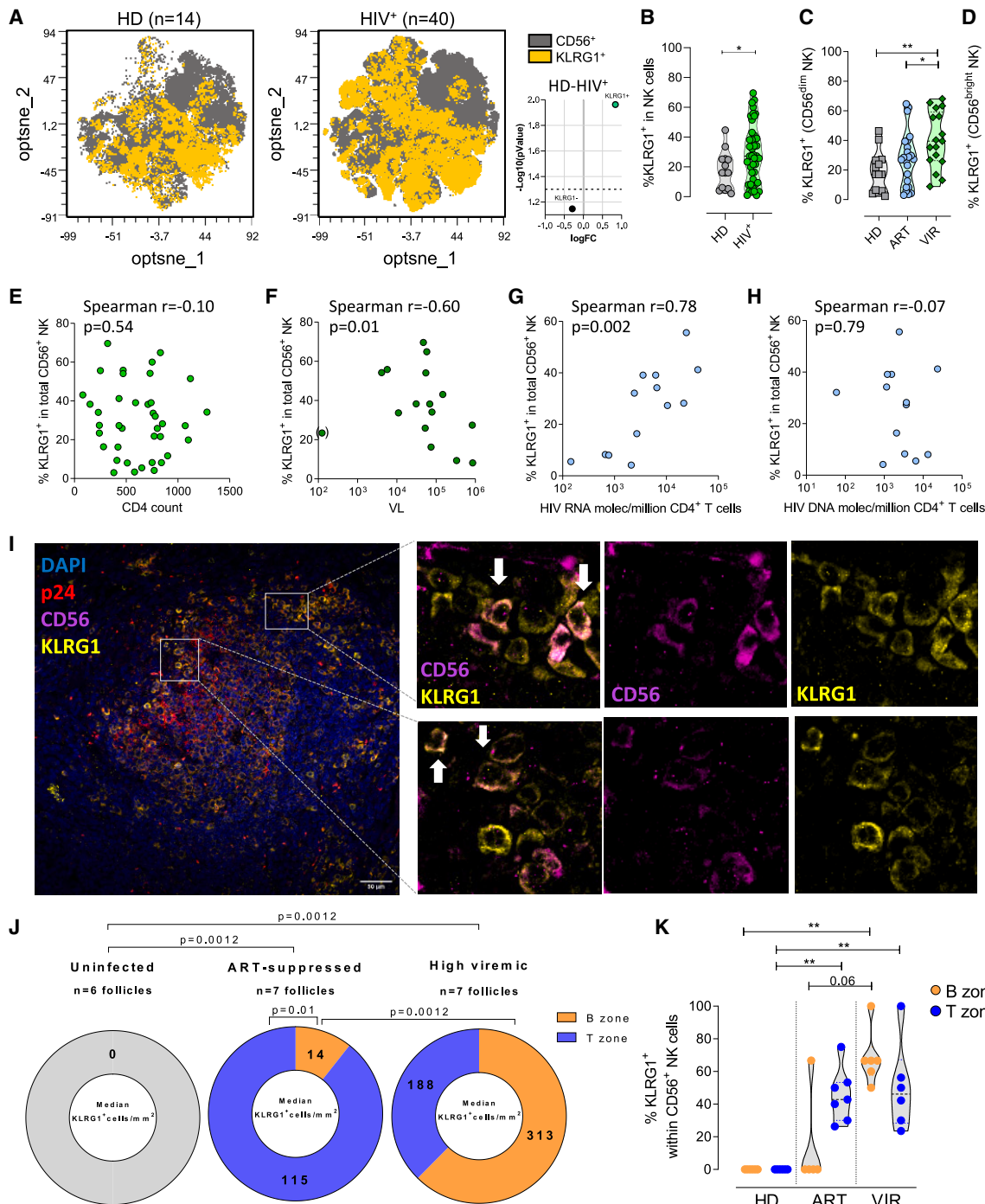


**Figure 1. Expression of KLRG1 in NK cells during HIV infection**

The expression of the KLRG1 receptor was measured by flow cytometry in different subjects.

(A) Opt-SNE plots showing the distribution of KLRG1<sup>+</sup> NK cells within the total pool of CD56<sup>+</sup> NK cells in HIV-negative donors (HD) and people with HIV (HIV<sup>+</sup>). The Volcano plot shows the difference in KLRG1 expression between both cohorts.

(B) Frequency of KLRG1<sup>+</sup> NK cells in a cohort of HD (n = 14) and PWH (n = 40).

(C) Percentage of KLRG1<sup>+</sup> NK in CD56<sup>dim</sup> NK cells in HD and in HIV<sup>+</sup> with detectable viral loads (VIR) or on antiretroviral treatment with suppressed viremia (ART).

(D) Percentage of KLRG1<sup>+</sup> NK in CD56<sup>bright</sup> NK cells in HD and HIV<sup>+</sup> in VIR or ART subjects. For (B), (C), and (D), median with range is represented. Statistical comparisons were performed using the Mann-Whitney test. \*p < 0.05; \*\*p < 0.01.

(legend continued on next page)

latency, proportions of total and CD16<sup>+</sup> NK cells correlated with decreasing levels of the total HIV reservoir size.<sup>13</sup> Of note, the exact mechanisms by which NK cells might target viral reservoirs are not fully understood.

It is widely accepted that a broad set of receptors expressed on the surface of NK cells dictate the variety of their effector responses. These receptors have activating or inhibitory potential, and the combination of their expression and signaling on NK cells delineates cell subsets with different capabilities.<sup>14,15</sup> However, how the expression and combination of these receptors are affected by different pathological settings and how this might influence health outcomes is largely unknown. Thus, elucidating the most potent NK cell subsets in PWH on ART and boosting them might significantly impact HIV persistence. Importantly, finding exhausted phenotypes, as in the case of CD8<sup>+</sup> T cells, might help to identify new targets for restoration of NK functionality.

Killer cell lectin-like receptor subfamily G member 1 (KLRG1) is a conserved C-type lectin inhibitory receptor expressed in different subsets of  $\gamma\delta$  T cells, CD4<sup>+</sup> T, CD8<sup>+</sup> T, NK, and Treg cells, whose role remains not fully understood.<sup>16–20</sup> KLRG1 expression seems to increase with age and as a consequence of unresolved chronic infections or tumor processes; and higher frequencies are found on antigen-experienced and differentiated cells.<sup>21–24</sup> Most of the studies on KLRG1 have focused on T cells, defining this molecule as a marker of cell senescence and differentiation.<sup>18,21–23,25</sup> However, KLRG1 has also been identified as an immune inhibitory checkpoint receptor. Indeed, KLRG1 possesses a tyrosine-based inhibitory motif (ITIM) in its cytoplasmic domain, conferring inhibitory potential.<sup>26–28</sup> Moreover, high KLRG1 expression stimulates signaling through protein sensors, such as the AMP-responsive protein kinase, which inhibit NK cell cytotoxicity and proliferation.<sup>29</sup> Other studies have shown that KLRG1 inhibits effector activity after the engagement with its cognate ligands, the E-, N-, and R-cadherins, present in target cells.<sup>30,31</sup> Thus, KLRG1 could represent an understudied negative regulatory receptor and, therefore, a new immunostimulatory target to explore in the context of HIV infection.

Here, we show that a significant fraction of NK cells in PWH expresses KLRG1, both in blood and lymph nodes, and its expression correlates with viral transcription during HIV persistence in treated infection. Phenotypic and functional analyses indicate that KLRG1-expressing NK cells represent a dysfunctional subset, with inferior capabilities to kill HIV-infected cells. Importantly,

immunotherapy against KLRG1 enhances the cytotoxic potential of NK cells against the HIV latent reservoir. Moreover, we demonstrate that KLRG1 is also expressed on CD4<sup>+</sup> T cells harboring inducible HIV and that anti-KLRG1 antibodies could be used for both, “shock” the HIV reservoir and potentiate the “killing” by NK cells. Thus, we identify KLRG1 as a target to exploit in HIV immunotherapies.

## RESULTS

### Active HIV transcription associates with higher frequencies of NK cells expressing KLRG1

We first studied the cell-surface expression of KLRG1 in a cohort of ART-suppressed (ART, n = 23) and viremic (VIR, n = 17) PWH (clinical data of participants #1–40 in Table S1) and compared it to healthy donors (HD, n = 14). An example of the gating strategy used for these analyses is shown in Figure S1. In total NK cells (CD3<sup>−</sup>CD56<sup>+</sup>), we found significantly higher frequencies of KLRG1 expression in HIV<sup>+</sup> individuals (VIR and ART) than in HDs (Figure 1A). KLRG1 was expressed with median values of 16.1% and 27.3% for HD and HIV<sup>+</sup>, respectively (Figure 1B). Also, we studied if KLRG1 expression was observed in the two main populations of NK cells according to their expression levels of CD56. Indeed, we found KLRG1 over-expression during untreated HIV infection (VIR) in CD56<sup>dim</sup> (Figure 1C) but also in less differentiated CD56<sup>bright</sup> NK cells (Figure 1D). Aging and some unresolved chronic infections have been linked to KLRG1 expression.<sup>23,24,29</sup> Importantly, VIR PWH showed higher KLRG1 levels, but no differences in age were observed between these cohorts (Table S1). Moreover, ART significantly reduced KLRG1<sup>+</sup> NK cells in both NK subsets from peripheral blood mononuclear cells (PBMCs) compared with VIR individuals, but there was a trend for no normalization of the KLRG1 values, especially for the CD56<sup>dim</sup> cells (median values of 17.0% and 27.3% for HD and ART, respectively) (Figure 1C). We next examined the relationship between clinical parameters during untreated HIV infection and the percentage of KLRG1<sup>+</sup> NK cells. We did not find a significant correlation with the absolute CD4<sup>+</sup> T cell counts (Figure 1E); however, we did observe a negative correlation between plasma viral load in VIR individuals and KLRG1 expression on NK cells (Figure 1F). We believe this correlation reflects the link between KLRG1 expression and unresolved chronic HIV infection, because samples with the highest viral loads were frequently obtained during early HIV infection

(E–H) Spearman correlations between the percentage of KLRG1<sup>+</sup> NK cells and (E) absolute CD4<sup>+</sup> T cell count, (F) viral load during untreated infection (n = 16) (dot in parentheses was not included for the statistical analysis), (G) HIV RNA molecules per million CD4<sup>+</sup> T cells during ART (n = 13), or (H) HIV DNA molecules per million CD4<sup>+</sup> T cells during ART (n = 13) are represented.

(I) Representative micrograph of a lymph node section from one HIV<sup>+</sup> VIR individual stained with anti-CD56 (purple), anti-KLRG1 (yellow), and anti-p24 (red) antibodies. White boxes indicate regions where NK cells show expression of both CD56 and KLRG1. The right panels correspond to zoomed views of CD56<sup>+</sup> KLRG1<sup>+</sup> cells.

(J) Graph showing the number of KLRG1<sup>+</sup> cells per mm<sup>2</sup> in the B and T zones from uninfected, ART-suppressed, and VIR lymph node samples. B and T cell zones were identified based on the intensity of the DAPI staining and the morphology of the cell nuclei.

(K) Frequency of KLRG1<sup>+</sup> cells within CD56<sup>+</sup> NK cells in the lymph nodes from an HD, a VIR (#42), and an ART-suppressed (#41) PWH. Each dot corresponds to one B cell follicle. The percentage of NK cells expressing KLRG1 in the B cell zone or the intrafollicular region and in the T zone or the extrafollicular region was represented in orange and blue dots, respectively. Median and min-max rank is represented. Intra-sample comparisons between values inside or outside the B cell follicles from HD, VIR, and ART were performed using the Wilcoxon test, and the inter-sample comparisons between PWH and HD were performed using the Mann-Whitney test.

See also Figures S1 and S2 and Table S1.

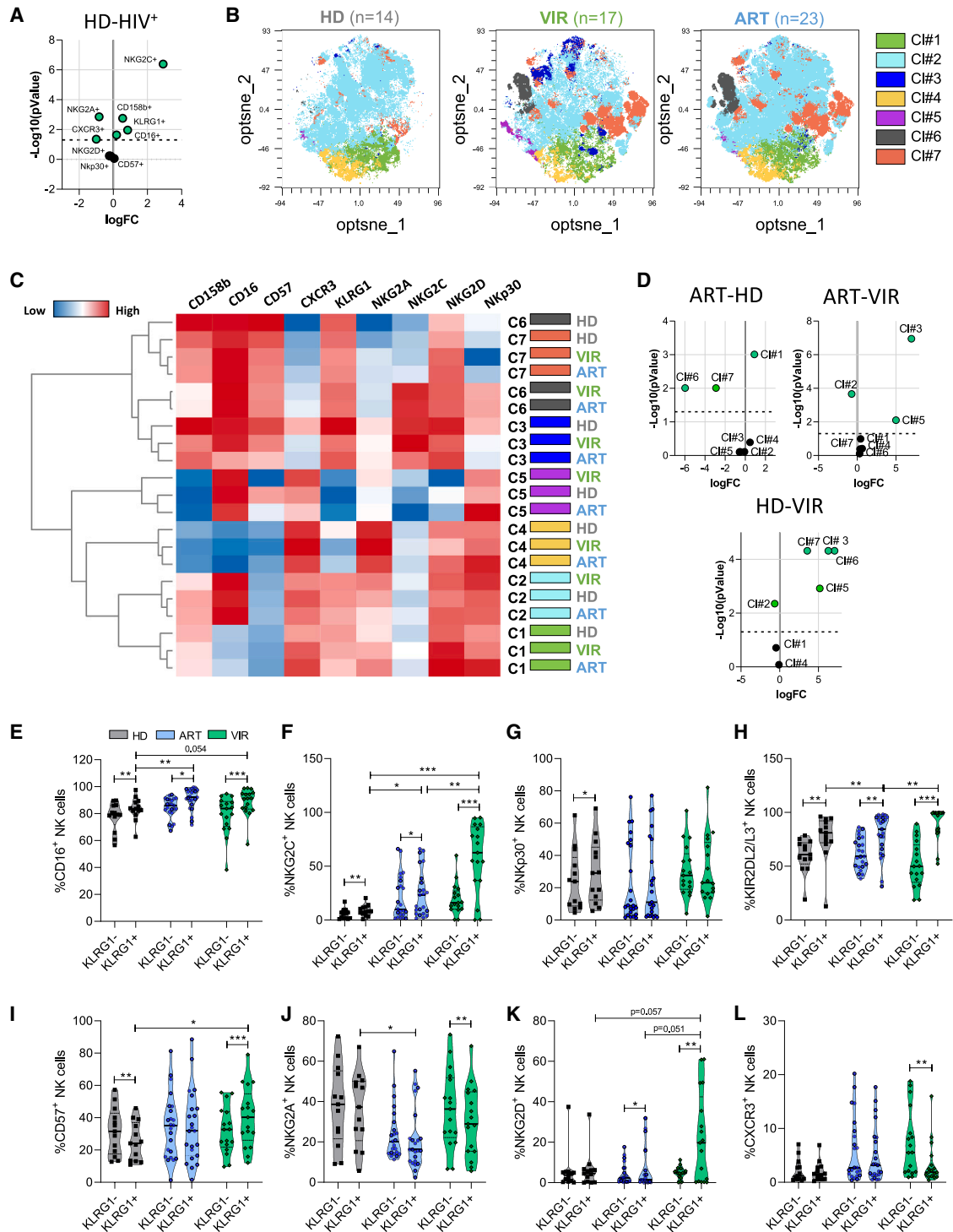


**Figure 2. Characterization of NK cells expressing KLRG1 in HIV infection**

The expression of different NK markers was quantified by flow cytometry in different subjects: healthy donors (HD) n = 14, HIV<sup>+</sup> viremic (VIR) n = 17, and HIV<sup>+</sup> ART-treated individuals (ART) n = 23.

(A) Volcano plot showing the statistically significant differences in the cluster composition between cohorts HIV<sup>+</sup> and HD.

(B) Reduction of dimensionality analysis of the expression of different receptors in total (CD56<sup>+</sup>) NK cells.

(C) Heatmap showing the differences in the mean fluorescence expression of the different NK cell receptors, in HD, VIR and ART cohorts, regarding the different cell clusters identified in Figure 2B and represented in different colors.

(legend continued on next page)

and, thus, with a limited time of viral replication. When we focused on ART-suppressed PWH, we found a significant direct correlation between intracellular viral RNA and the expression of KLRG1 on NK cells (Figure 1G). By contrast, no association was found between KLRG1 and the total HIV reservoir size, measured as the total viral DNA within the CD4<sup>+</sup> T population (Figure 1H).

Next, we examined the presence and localization of KLRG1<sup>+</sup> NK cells in the lymph nodes, for which the follicles are a privileged anatomical site for HIV persistence.<sup>32</sup> We performed immunostaining of the HIV protein p24, the NK cell receptor CD56, and KLRG1 in anatomically intact lymph node tissue preparations from one uninfected control and two PWH (ART-suppressed #41 and VIR #42, Table S1). As shown in Figures 1I, S2A and S2B, p24 showed the typical two-staining pattern observed in the B cell follicles,<sup>33</sup> network-like staining probably corresponding to virions captured by follicular dendritic cells, and cells with a more dense spherical signal indicating productive HIV infection (Figure S2B). In general, changes in the total number of NK cells (CD56<sup>+</sup>) were not detected in lymph nodes from PWH compared to the uninfected control (Figure S2C). However, we observed an increase in the total number of cells expressing KLRG1 in lymph nodes from the two PWH studied, both in the T and B zones (Figures 1I, 1J, and S2A). Notably, high frequencies of KLRG1<sup>+</sup> NK cells were observed in the lymph nodes of PWH; the increase of NK cells expressing KLRG1 was particularly significant in the B zone of the VIR individual (Figures 1J and 1K). Of note, the ART sample showed higher expression of KLRG1 on NK cells located in the T zone, but not in the B zone, of the lymph nodes compared with the negative control. We speculate that the disorganization of the B cell follicle after HIV infection might allow NK cells to better penetrate the B cell follicle. Alternatively, it is possible that HIV infection accumulates NK cells expressing CXCR5 in lymph nodes, the receptor that directs the entry of immune cells into the B cell follicle. This has been shown before in samples from PWH<sup>34</sup> and in samples from a non-human primate model of viral control.<sup>35</sup>

Overall, our results show the existence of a significant fraction of NK cells with expression of KLRG1 both in the blood and within the lymph nodes of PWH, which is compatible with persistent HIV infection. Importantly, during ART, the expression of KLRG1 correlates with active HIV transcription in blood, and a significant expression of KLRG1 on NK cells remains in lymph nodes.

### HIV infection expands different populations of NK cells expressing KLRG1, and more differentiated cells are maintained after ART

We studied if NK cells expressing KLRG1 had a different expression pattern of important receptors for NK activity. For these analyses, we included NK receptors with activating or inhibitory potential upon interaction with ligands found on

HIV-infected cells (CD16, NKG2C, NKG2A, NKG2D, NKp30, and KIR2DL2/L3), the maturation marker CD57, and the chemokine receptor CXCR3 (illustration in Figure S2D). In general, we observed that HIV<sup>+</sup> PWH had higher expression of KLRG1, but also they expressed more NKG2C, CD16, and CD158b (Figure 2A). We then performed a reduction of dimensionality analysis with the data of the individual cohorts. Unsupervised clustering analysis using FlowSOM algorithm allowed us to identify seven different NK cell clusters with a particular expression of the selected receptors in cells expressing KLRG1 (Figure 2B). Specifically, clusters #1 and 2 identified subpopulations of NK cells with medium expression levels of KLRG1, whereas clusters #3, 6, and 7 were populations with high expression of KLRG1 (Figure 2C). Interestingly, these clusters with high expression of KLRG1 were mainly apparent after HIV infection (Figures 2B and 2D). These populations were also characterized by an increased expression of CD16, an important activating receptor to mediate ADCC, elevated levels of NKG2D, CD57, and the inhibitory receptors KIR2DL2/L3 (KIR CD158b), together with mid-low expression of NKG2A (Figures 2C and S3). We also evaluated the impact of ART on these NK populations. It has been extensively documented that HIV infection alters the expression of NK receptors and function, and ART does not fully revert these alterations.<sup>6,7</sup> Statistical comparison within NK clusters between all cohorts is depicted in Figure 2D. In general, clusters #6 and 7 were not normalized after treatment compared to HDs, and high expression of these clusters is still present after ART (Figure 2D). Importantly, cluster #6 showed a significant increase in the expression of NKG2C only upon HIV infection that was not normalized upon ART (Figures 2C and S3). Finally, we also performed a more traditional analysis of the percentages of expression of the different markers in both populations, with and without expression of KLRG1. An example of the gating strategy used is shown in Figure S1. The results largely confirmed the above main conclusions obtained with the reduction of dimensionality analysis and showed that cells expressing KLRG1 have higher levels of CD16, NKG2C, KIR, CD57, and NKG2D and lower levels of NKG2A and CXCR3, especially in VIR individuals (Figures 2E–2L). Moreover, ART was able to normalize some of the populations, but high expression of CD16, NKG2C, and KIR (Figures 2E, 2F and 2H) and low expression of NKG2A (Figure 2J) were still present in the KLRG1<sup>+</sup> subpopulation after ART.

Overall, we observe that HIV infection expands populations of NK cells expressing KLRG1 with memory-like features (NKG2C<sup>+</sup>), high expression of the inhibitory KIR CD158b, the differentiation marker CD57, and the activating receptor NKG2D, and low levels of the inhibitory NKG2A receptor. The lower expression of CXCR3 would indicate that these KLRG1<sup>+</sup> cells are less able to migrate toward a CXCL9/10/11 gradient.<sup>36</sup> Importantly, ART does not normalize all these KLRG1<sup>+</sup>

(D) Volcano plots showing the statistically significant differences in the cluster composition between cohorts.

(E–L) Percentage of expression of different receptors in KLRG1<sup>+</sup> and KLRG1<sup>-</sup> NK cells. All graphs represent the median and ranges. Statistical comparisons intra-cohort were performed using the Wilcoxon matched-pairs signed-rank test, and comparisons inter-cohort used the Mann-Whitney test. \*p < 0.05; \*\*p < 0.01; \*\*\*p < 0.001.

See also Figures S1, S2, and S3 and Table S1.

populations, and they keep representing a substantial proportion of cells with more frequent activated receptors and differentiated phenotypes.

### KLRG1<sup>+</sup> NK cells are functionally impaired in samples from ART individuals

As a next step, we aimed to directly elucidate the functional signatures of KLRG1<sup>+</sup> NK cells. We focused on the cohort of ART subjects as important candidates for a potential functional cure of HIV. First, we performed NK recognition assays against the MHC-I-deficient cell line K562, using unstimulated NK cells or primed with IL-15 (gating strategy shown in Figure S4A) (NK cells from participants #10, 13–16, 18, 19, 43–45 in Table S1). In general, NK cells from ART individuals were able to kill the cell line K562 (Figure S4B). Dimensionality reduction analysis identified six clusters in the NK cell population, from which clusters #1, 4, and 5 were significantly expanded upon the cell target challenge and IL-15 cytokine stimulation (Figures 3A, 3B, and S5A). These clusters comprised cells with a strong cytotoxic profile, expressing the lysosomal-associated membrane protein-1 CD107a, IFN- $\gamma$  (Figure 3C), and the activation marker CD69 (Figure 3D). Of note, clusters #1 and 4 widely expressed KLRG1 (Figure 3E), and showed enriched expression of CD57, NKG2C, and CD16 (Figure 3F). Subsequently, we performed a comparative functional analysis and studied the cytotoxic response of NK cells, expressing or not the KLRG1 receptor, stimulated with IL15, and after co-culturing with the MHC-I-devoid cell line K562. We observed that KLRG1<sup>+</sup> NK cells expressed more HLA-DR and CD69 than their negative counterparts (Figures 3G and 3H). NK cells expressing KLRG1 exhibited a lower degranulation response (Figures 3I and 3J), lower frequencies of IFN- $\gamma$  producing cells (Figure 3K), and fewer polyfunctional CD107a<sup>+</sup>IFN- $\gamma$ <sup>+</sup> cells (Figure 3M) compared to the negative KLRG1 fraction. Results from NK cells in the absence of the target cells or without previous IL-15 stimulation are shown in Figures S5B–S5H. Overall, we showed that KLRG1<sup>+</sup> NK cells produce functional molecules, such as IFN- $\gamma$  and CD107a, upon interaction with K562 targets; however, these cells are functionally more impeded than cells not expressing the KLRG1 receptor.

### Antibody intervention enhances the cytotoxic potential of KLRG1<sup>+</sup> NK cells at killing HIV-infected cells

Antibody therapies intended to block different immune checkpoints to reinvigorate the effector functions of immune cells are promising new therapies, especially against tumor cells.<sup>37</sup> Thus, we tested if anti-KLRG1 antibodies might enhance functionality of NK cells from ART individuals. To test if targeting KLRG1 inhibits the exhausted phenotype, we cultured isolated NK cells from different ART-suppressed PWH (participants #46–51, Table S1) for 4 h in the presence of a specific anti-KLRG1 antibody. We measured cell activation, degranulation, and IFN- $\gamma$  secretion. The co-culture of NK cells with HIV-infected cell targets in the presence of the anti-KLRG1 antibody significantly increased the frequency of IFN- $\gamma$ -producing cells in the CD56<sup>dim</sup> subset expressing the KLRG1 receptor (Figure 4A) but not in non-expressing KLRG1 cells (Figure 4B). More notably, targeting KLRG1 did not change the frequency of cells with the

potential to degranulate, but it strongly triggered a degranulation response (mean fluorescence intensity [MFI] CD107a<sup>+</sup>) in less differentiated CD56<sup>bright</sup> NK cells (median of 3,820 vs. 7,686 in the presence of the isotype control IgG2 and anti-KLRG1 Ab, respectively) (Figure 4C). No changes in the degranulation capacity were observed in KLRG1<sup>-</sup> NK cells (Figure 4D). We included in these experiments controls of NK cells cultured with phorbol myristate acetate (PMA)+ionomycin (Figures S6A–S6D). Thus, we show that targeting KLRG1 significantly increases the functionality of this subset.

Next, we performed NK-killing assays after antibody engagement. *Ex vivo* infected CD4<sup>+</sup> T cells were subjected to autologous NK natural cytotoxicity assays after engagement with anti-KLRG1 or control antibodies (participants #52–57, Table S1). Purity of the isolated NK cells was >94% (Figure S6E). We calculated cell killing as the reduction in the percentage of virally infected cells. A representative gating strategy is shown in Figure S6F. Targeting KLRG1 in NK cells significantly enhanced the killing of the total pool of HIV-infected cells (Figure 4E). Likely, the enhanced effector response achieved by the anti-KLRG1 antibody was specific to the KLRG1<sup>+</sup> NK cell subpopulation, since the blockade of Fc receptors on the NK cells, which potentially masks unspecific interactions through its constant fraction (Fc), showed no effect on the overall cell killing induced by the KLRG1 antibody. No effect was observed after incubation with the isotype control (Figure S6G). Another potential benefit of targeting KLRG1 might be the masking of the interaction between this receptor with its ligands. Thus, we tested if HIV infection upregulated the KLRG1 ligand E-cadherin, a molecule known to restrain the NK function through KLRG1 engagement.<sup>28</sup> To this end, we performed the *ex vivo* infection of isolated CD4<sup>+</sup> T cells (participants #52–57 in Table S1) and assessed the expression of the E-cadherin by flow cytometry on infected (p24<sup>+</sup>) CD4<sup>+</sup> T cells. Although a consistent increment was observed in all experiments, the expression of E-cadherin on infected cells was very low with the exception of two samples (Figure 4F). Of note, we have not assessed if these E-cadherin-positive cells were preferentially infected or if HIV induced its upregulation, but blocking the low levels of E-cadherin expression after HIV infection induced a small improvement in the NK capacity to kill HIV-infected cells (Figure S6H). Other immune cell populations present in PBMCs such as monocytes have been shown to express high levels of E-cadherin,<sup>38</sup> which could potentially restrain KLRG1<sup>+</sup> NK cells. Also, high levels of soluble E-cadherin have been found in PWH,<sup>39</sup> further supporting the potential *in vivo* benefits of an antibody targeting the KLRG1 immune checkpoint. Finally, we directly measured the response of KLRG1-expressing NK cells to HIV<sup>+</sup> cell targets (participants #58–61 in Table S1). For that, we performed autologous co-cultures between previously isolated KLRG1<sup>+</sup> NK cells or KLRG1<sup>-</sup> NK cells by fluorescence-activated cell sorting (FACS) and *ex vivo* HIV-infected CD4<sup>+</sup> T cells. KLRG1<sup>+</sup> NK cells that were incubated with the anti-KLRG1 antibody showed a more robust cytotoxic response against HIV-infected targets by both mechanisms, the natural cytotoxicity and the ADCC, than NK cells lacking the expression of KLRG1 (Figures 4G and 4H). In general, KLRG1<sup>+</sup> NK cells stimulated with the anti-KLRG1 antibody

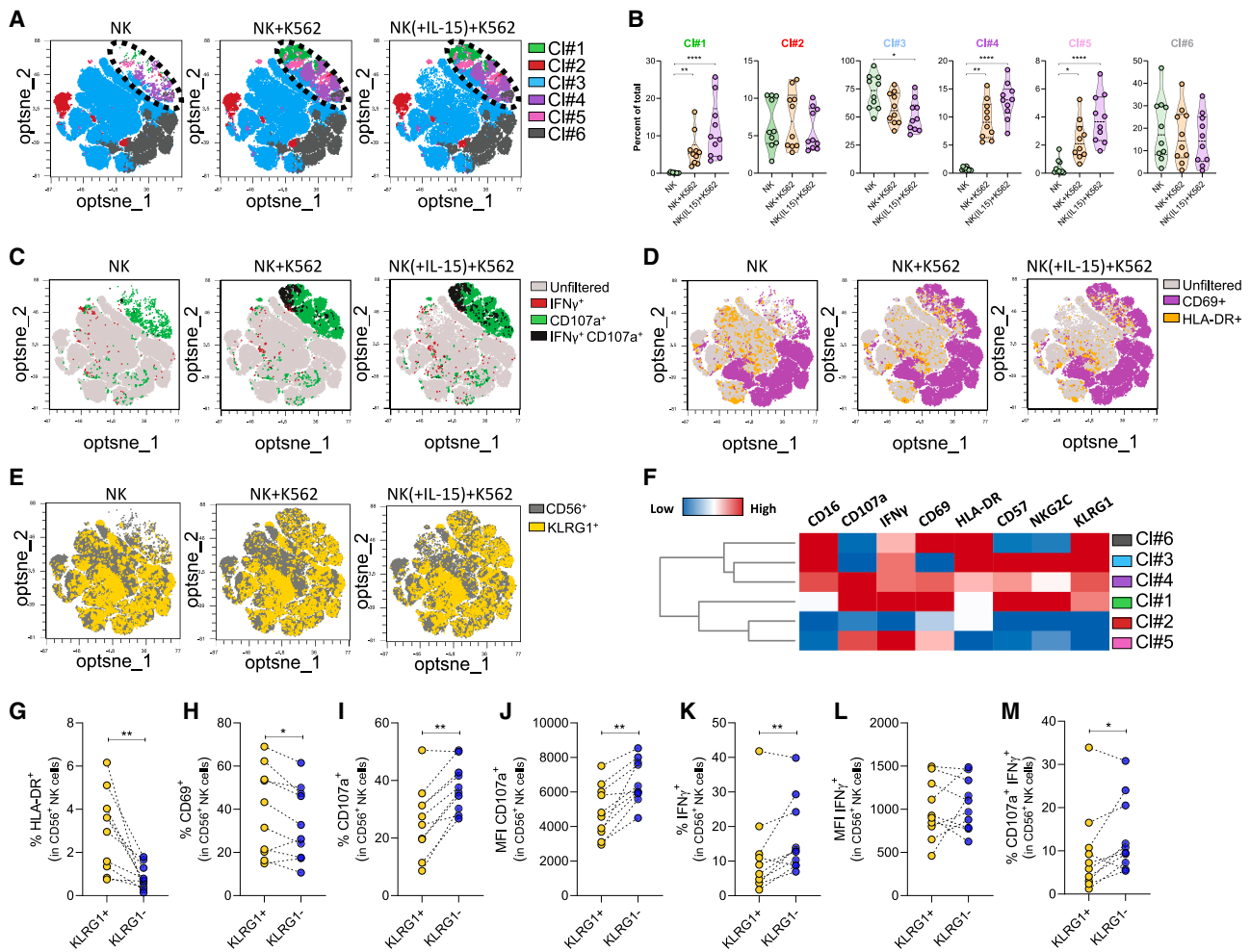


**Figure 3. Functional profile of KLRG1<sup>+</sup> NK cells in ART-suppressed PWH**

MHC-I-devoid K562 cells were subjected to NK-killing assays (n = 10). Functional markers were measured by flow cytometry under different conditions.

(A) Reduction of dimensionality analysis for the expression of KLRG1, CD57, CD16, NKG2C, HLA-DR, CD69, IFN- $\gamma$ , and CD107a in total (CD56<sup>+</sup>) NK cells. Three conditions are represented: NK alone, NK + K562, and NK (IL15) + K562.

(B) Violin graphs showing the frequency of the different clusters of NK cells identified in (A). Statistical comparisons were performed using the Kruskal-Wallis test when required. \*p < 0.05; \*\*p < 0.01; \*\*\*p < 0.001; \*\*\*\*p < 0.0001.

(C) Expression of CD107a and IFN- $\gamma$  on the different clusters identified in (A).

(D) Expression of CD69 and HLA-DR on the different clusters identified in (A).

(E) Expression of KLRG1 on the different clusters of NK cells identified in (A).

(F) Heatmap showing the intensity of expression of the different markers on the NK clusters represented in different colors.

(G–I) Percentage (G) of HLA-DR<sup>+</sup> cells in total CD56<sup>+</sup> KLRG1<sup>+</sup> (yellow) or KLRG1<sup>-</sup> (blue) NK cells, after co-culturing with the K562 target cells and with the additional IL-15 stimulus. Similarly, the values of other parameters are represented in (H) frequency of CD69<sup>+</sup> cells and (I) percentage of cells expressing the CD107a degranulation marker.

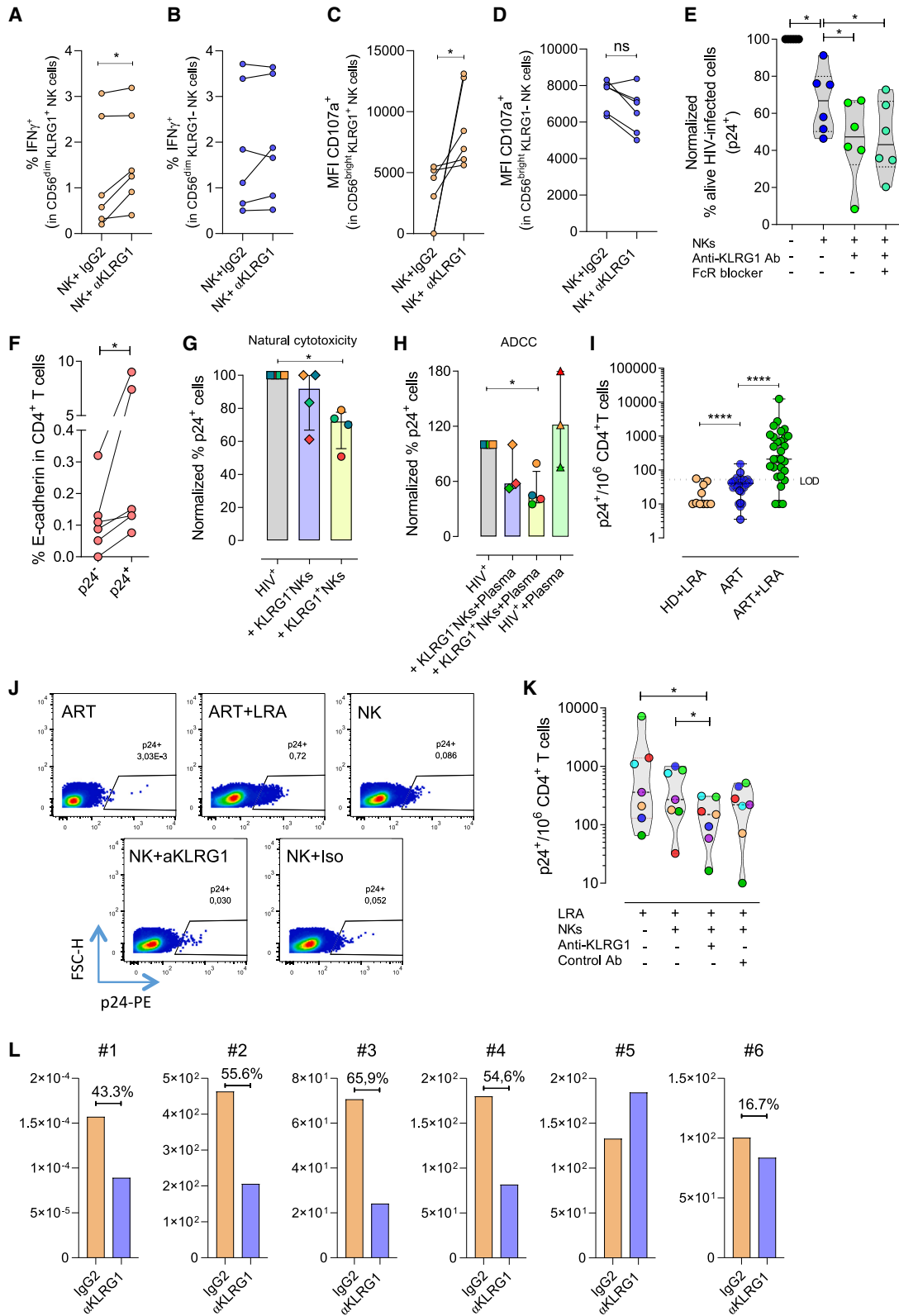
(J–M) Mean fluorescence intensity (MFI intensity) signal (J) for CD107a expression, (K) frequency of cells producing IFN- $\gamma$ , (L) MFI for IFN- $\gamma$ , and (M) percentage of polyfunctional, double-positive CD107a<sup>+</sup>IFN- $\gamma$ <sup>+</sup> cells. Statistical comparisons were performed using Wilcoxon matched-pairs signed-rank test. \*p < 0.05; \*\*p < 0.01; \*\*\*p < 0.001; \*\*\*\*p < 0.0001.

See also [Figures S4](#) and [S5](#) and [Table S1](#).

had the ability to kill approximately 20% more infected cells than their negative counterparts.

Last, we tested if targeting KLRG1 induces an NK-mediated cytotoxic response against viral-reactivated cells from the natural reservoir. We performed functional NK assays using samples from seven ART-suppressed PWH after reactivation (participants #23, 65–70, [Table S1](#)). Detection of p24 was first evaluated

in samples from HDs and ART-treated PWH after viral reactivation. The limit of detection was set up at 53 copies/million cells calculated by the formula 3\*SD of the mean percentage of p24<sup>+</sup> cells detected in HD samples. As previously reported,<sup>40</sup> we observed viral reactivation of dormant HIV ([Figures 4I](#) and [S6I](#)). Notably, the incubation with KLRG1-directed antibodies strongly enhanced the NK-mediated killing of the total pool of



(legend on next page)

viral-reactivated cells (median reduction in p24<sup>+</sup> cells of 75.15%). This effect was not observed with the control antibody (Figures 4J and 4K). Moreover, we performed the intact proviral DNA assay in the remaining CD4<sup>+</sup> T cells in additional samples from six ART individuals (participants #71–76, Table S1). Reduction in the intact proviruses was observed in five out of six samples tested (Figure 4L). Altogether, we show that targeting KLRG1 restores the functional abilities of NK cells and enhances the capacity to kill HIV-infected cells by both natural cytotoxicity and ADCC and to reduce the natural HIV reservoir after viral reactivation.

### KLRG1 is expressed on CD4<sup>+</sup> T cells harboring inducible HIV genomes, and the anti-KLRG1 antibody induces viral reactivation

Major efforts in the HIV field are directed at finding efficient compounds for both reactivating latently HIV-infected cells and stimulating the immune system of PWH to eliminate HIV reservoirs. Therapeutic strategies integrating these two steps are designated as a “shock and kill” approach.<sup>11</sup> For assessing the suitability of using KLRG1 in this approximation, we studied the feasibility of using anti-KLRG1 monoclonal antibodies as LRAs. First, we checked the expression of KLRG1 in CD4<sup>+</sup> T cells from a cohort of VIR and ART-suppressed PWH (participants #1–40 Table S1), and we found a median of 23.6% and 19.4% of these cells expressed the KLRG1 receptor, respectively (Figure 5A). Moreover, in ART individuals, the expression of KLRG1 on CD4<sup>+</sup> T cells directly correlated with the intracellular levels of HIV RNA (Figure 5B). Interestingly, the targeting of KLRG1 in CD4<sup>+</sup> T cells with directed antibodies significantly increased the number of viral RNA molecules (median fold increase of 3.2), indicating viral reactivation (Figure 5C) (participants #1, 2, 4–6, 9, 12, 62–64 Table S1). Romidepsin was used as a control for viral reactivation (Figure S6J). This suggests that KLRG1 may identify a fraction of CD4<sup>+</sup> T cells with latent HIV and/or induce higher levels of HIV RNA from transcriptionally active

HIV-infected cells. We then assessed the content of total HIV DNA in KLRG1<sup>+</sup> and KLRG1<sup>−</sup> CD4<sup>+</sup> T cells isolated by FACS from samples of four ART-suppressed PWH (participants #58–61 Table S1). We were able to detect HIV in KLRG1-expressing cells, with similar levels to those observed in the negative KLRG1 population (Figure 5D). Moreover, in lymph node samples from PWH (both VIR and ART suppressed), we observed cells in the follicles productively infected (dense intracellular p24 staining) and concomitantly expressing KLRG1 on the surface (Figures 5E and S6K). These results indicate that KLRG1 might be found in productively HIV-infected cells. Next, we studied if *ex vivo* HIV infection upregulates the expression of KLRG1 on CD4<sup>+</sup> T cells (gating strategy shown in Figure S7). We found a slight increase in the expression of this receptor, but not in the intensity of expression, upon infection with the HIV<sub>BaL</sub> strain (Figure 5F), which was not observed with HIV<sub>NL4.3</sub> (Figure 5G). This suggests that KLRG1 is not selectively induced upon acute HIV infection in CD4<sup>+</sup> T cells. Differences between both viral strains might be due to the preferential infection of the BaL isolate for memory CD4<sup>+</sup> T cells expressing KLRG1, as previously observed for the PD-1 molecule.<sup>41</sup> Overall, our data support the potential of targeting KLRG1 to reactivate the latent HIV reservoir, more likely in combination with other LRAs.

### DISCUSSION

One of the major obstacles to curing HIV is the presence of HIV reservoir cells with limited immune recognition, in part due to the development of immune resistance mechanisms, and the impaired effector function of immune cells.<sup>5,40,42–44</sup> NK cells are lymphocytes of the innate immunity with superior capabilities to kill viral-infected cells. HIV infection, however, alters different immune compartments, including NK cells. Hallmarks of this viral infection are the expansion of certain subsets of NK cells, persistent immune activation, and a reduced capacity to perform ADCC, which are not fully

#### Figure 4. Targeting KLRG1 increases the functional capabilities of NK cells

NK cells were cultured with *ex vivo* infected CD4<sup>+</sup> T cells after stimulation with the anti-KLRG1 antibody. Functional parameters on NK cells and direct cell killing of the HIV<sup>+</sup> targets were quantified by flow cytometry.

(A–D) Frequency (A) of IFN- $\gamma$ <sup>+</sup> cells in NK KLRG1<sup>+</sup> cells, (B) frequency of IFN- $\gamma$ <sup>+</sup> cells in NK KLRG1<sup>−</sup> cells, (C) mean fluorescence intensity (MFI) of CD107a in KLRG1<sup>+</sup> cells, and (D) MFI of CD107a in KLRG1<sup>−</sup> cells.

(E) Reduction in p24<sup>+</sup> after co-culturing *ex vivo* HIV-infected CD4<sup>+</sup> T cells with NK cells previously stimulated with the anti-KLRG1 antibody. Fc blocker is shown as a control.

(F) Expression of the molecule E-cadherin on CD4<sup>+</sup> T cells in infected (p24<sup>+</sup>) and uninfected (p24<sup>−</sup>) cells after *ex vivo* HIV infection.

(G) Natural cytotoxicity assay of *ex vivo* HIV-infected CD4<sup>+</sup> T cells after co-culturing with isolated NK expressing or not the KLRG1 and stimulated with the anti-KLRG1 antibody.

(H) ADCC assay of *ex vivo* HIV-infected CD4<sup>+</sup> T cells after co-culturing with isolated NK expressing or not the KLRG1 and stimulated with the anti-KLRG1 antibody. The condition with plasma from an HIV-positive person is shown as a control. In (G) and (H), the CD4<sup>+</sup> T cells and NK cells were isolated by FACS.

(I) P24<sup>+</sup> cells in samples from ART-suppressed PWH at baseline and after viral reactivation with PMA/ionomycin (LRA). The limit of detection is set up at 53 copies/million cells calculated by the formula 3\*SD of the mean percentage of p24<sup>+</sup> cells detected in healthy donor (HD) samples.

(J) Functional NK assays after reactivation of the natural latent HIV reservoir of isolated CD4<sup>+</sup> T cells from ART-treated PWH. P24<sup>+</sup> cells are quantified by flow cytometry as a measure of viral reactivation. This panel shows an example of the p24 staining.

(K) Functional NK assays after reactivation of the natural latent HIV reservoir of isolated CD4<sup>+</sup> T cells from ART-treated PWH. Summary graph for p24 levels in CD4<sup>+</sup> T cells after the NK-killing assays. Palivizumab was used as a control antibody.

(L) Intact proviral DNA assay (IPDA) in samples from six ART-suppressed subjects after performing the NK-killing assay with primary *ex vivo* reactivated CD4<sup>+</sup> T cells with PMA and ionomycin and isolated NK cells. NK cells were treated with the anti-KLRG1 antibody or the isotype control IgG2. Percentages of intact proviral reductions are shown for each subject. Statistical comparisons were performed using the Wilcoxon matched-pairs signed-rank test, Friedman test, or Kruskal-Wallis test when required. \*p < 0.05; \*\*p < 0.01; \*\*\*p < 0.001; \*\*\*\*p < 0.0001.

See also Figure S6 and Table S1.

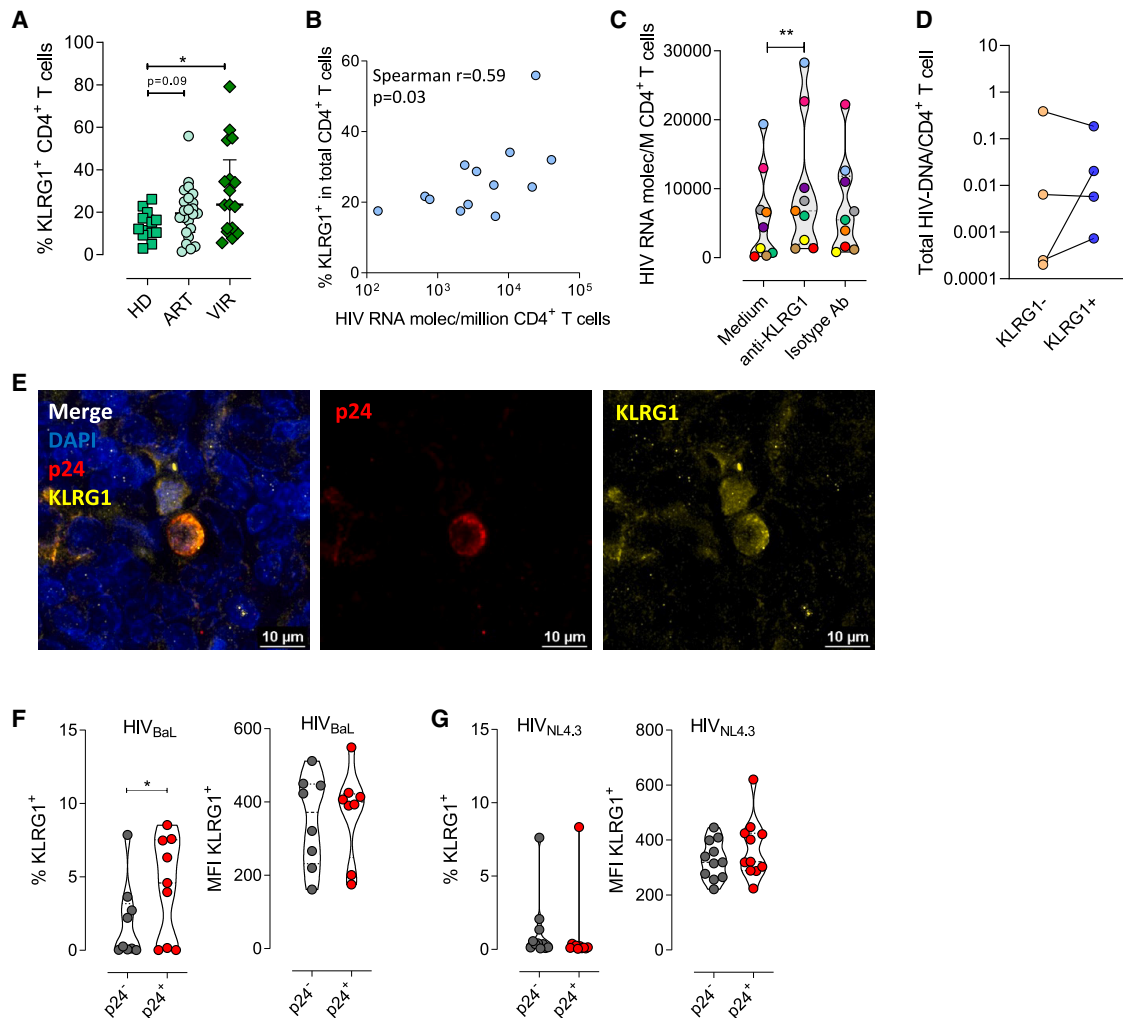


**Figure 5. Impact of targeting KLRG1 in CD4<sup>+</sup> T cells and in the viral reservoir**

(A) Frequency of KLRG1<sup>+</sup> CD4<sup>+</sup> T cells in a cohort of healthy donors (HD, n = 13), viremic (VIR, n = 17), and ART-suppressed (n = 23) PWH measured by flow cytometry.

(B) Spearman correlation between the percentage of KLRG1<sup>+</sup> CD4<sup>+</sup> T cells and the intracellular levels of HIV RNA.

(C) Intracellular HIV RNA levels measured by qPCR in CD4<sup>+</sup> T cells from ART PWH after stimulation with the anti-KLRG1 antibody or the isotype control antibody (n = 10).

(D) Quantification by qPCR of total HIV DNA in KLRG1<sup>+</sup> and KLRG1<sup>-</sup> CD4<sup>+</sup> T cells isolated by FACS (n = 4).

(E) Representative image of a lymph node section from a VIR HIV-infected PWH (#42). p24 HIV protein is shown in red and KLRG1 in yellow.

(F and G) Percentage and mean fluorescence intensity expression of KLRG1 in cells infected *ex vivo* with the HIV<sub>BaL</sub> strain (n = 9) or (G) the HIV<sub>NL4.3</sub> strain (n = 11). Statistical comparisons were performed using the Wilcoxon matched-pairs signed-rank test or Friedman test when required. \*p < 0.05, \*\*p < 0.01.

See also [Figures S6](#) and [S7](#) and [Table S1](#).

reverted even after ART-mediated viral control is achieved.<sup>7</sup> Thus, the development of new NK-targeted therapies to reinvigorate their functionality might influence HIV persistence.<sup>4,6,12,45</sup> One potential approach currently being explored is the targeting of NK receptors that restrain cell activity. In the present study, we report that HIV infection expands NK cell subpopulations imprinted with upregulated levels of the inhibitory receptor KLRG1, which have signs of advanced differentiation and impaired activity. Furthermore, ART does not reduce these impaired NK cells. Importantly, we show that targeting the KLRG1 receptor both induces viral reactivation in

CD4<sup>+</sup> T cells and reverses NK immune exhaustion favoring the elimination of HIV reservoir cells.

Here, we add evidence for the impact of chronic HIV infection on NK cells. We observe the upregulation of KLRG1 on NK cells during untreated and treated infection in both the PBMCs and the lymph nodes. This is concordant with previous findings showing KLRG1 expression on T and NK cells in chronic conditions, such as other viral infections and cancer.<sup>23,24,46,47</sup> The lymph nodes are a preferential anatomical sanctuary site for HIV persistence and contain a high burden of reservoir cells with transcriptionally active HIV.<sup>32</sup> Active viral transcription,

which has been associated with elevated levels of immune activation, might explain the high expression levels of KLRG1 on NK cells observed within the B cell follicles of PWH. In line with this, we observed a direct correlation between HIV transcription within CD4<sup>+</sup> T cells and KLRG1 expression on NK cells from blood. Similarly, augmented levels of KLRG1 have been reported in circulating and hepatic NK cells associated with hepatitis B infection,<sup>46</sup> and interestingly, the expression of KLRG1 on NK cells has been reported to respond to cell-intrinsic factors such as cell division and development,<sup>25</sup> to exposure to certain cytokines such as IFN- $\alpha$  or IL-12,<sup>25</sup> or to even specific treatments such as hydroxychloroquine.<sup>48</sup> Beyond the NK compartment, this receptor is also upregulated on virus-specific CD8<sup>+</sup> T lymphocytes during persistent HIV, Epstein-Barr virus, and cytomegalovirus infections.<sup>23,24</sup> Thus, our data and previous evidence suggest that the expression of KLRG1 could be induced on several immune cells following persistent infections.

We also found that KLRG1 expression is largely restricted to the CD56<sup>dim</sup> NK subset in uninfected subjects. However, HIV infection strongly increases KLRG1 levels in the CD56<sup>bright</sup> subpopulation. In general, CD56<sup>dim</sup> cells exhibit a more cytolytic profile, whereas CD56<sup>bright</sup> cells are known to produce large amounts of cytokines and have enhanced proliferative capacity, being both arms required for viral immune control.<sup>49</sup> Upregulation of the inhibitory KLRG1 on CD56<sup>bright</sup> NK cells has been previously observed in chronically infected HCV<sup>+</sup> individuals.<sup>38</sup> Moreover, it has been negatively associated with the potency of the immune responses against HPV16 and the progression of cervical intraepithelial neoplasia.<sup>50</sup> Our data point to HIV as a potent trigger for KLRG1 expression in CD56<sup>bright</sup> cells. Based on that, we believe that strategies reverting the KLRG1 expression on this specific NK subset may be particularly beneficial.

NK cells exhibit a diversity of phenotypes and functions, which are susceptible to high plasticity.<sup>15</sup> Our analyses show that KLRG1 distinguishes NK populations with elevated expression of important receptors involved in the differentiation and regulation of their function, such as CD57, CD16, NKG2C, and KIRs. Concordantly, it has been shown that mature NK cells express high levels of KLRG1.<sup>25</sup> Specifically, CD16 has a strong activating potential and allows NK cells to mediate ADCC activity. Published data support the relevant role of ADCC in the control of HIV and SIV infection and in shaping the viral reservoir during treated infection.<sup>40,51,52</sup>

We also find that HIV infection impacts the phenotype of KLRG1<sup>+</sup> NK cells significantly increasing the expression of the NKG2C receptor. This is noteworthy since this receptor is, in part, governing the tolerance or the reactivity of the NK cells toward the target cell; NKG2C provides activating signaling upon engaging its ligand, the HLA-E, expressed on the target cell. Moreover, NKG2C expression has been linked to memory-like features, particularly in CMV infection.<sup>53</sup> Importantly, ART does not normalize most KLRG1<sup>+</sup> NK populations, and cells expressing high levels of NKG2C are particularly persisting. We speculate that these cells may represent a new subpopulation of NK cells generated in response to HIV infection with features of memory cells, as previously reported for CMV infection.<sup>53</sup> Concordantly, a recent study has identified KLRG1 as a marker

of NK cells with immune memory attributes in HCV-infected individuals.<sup>54</sup>

Hallmarks for NK dysfunctionality are considered decreased NK effector functions such as natural cytotoxicity, as well as reduced IFN- $\gamma$  secretion and degranulation.<sup>55</sup> Here we observe that KLRG1<sup>+</sup> NK cells are functionally impaired when stimulated with K562 cell line targets. While we cannot rule out the possibility that the difference in function between the KLRG1-positive and -negative cells is due to differences in triggering of other NK cell receptors that affect cell function, the K562 data along with the HIV-infected cell killing assays is suggestive that NK cells expressing KLRG1 are in a state of functional exhaustion. This concurs with a prior report showing that prolonged NK stimulation leads to functional cell exhaustion with increased expression of KLRG1, among other factors.<sup>56</sup> Thus, we wanted to test if immune checkpoint blockade directed to KLRG1 could reprogram NK cell activation and boost a strong immune response against HIV-infected cells. Checkpoint blockade therapy, with PD-1 and its cognate ligand as the most studied targets, has demonstrated great benefit at reinvigorating exhausted cytotoxic T cells in several cancers.<sup>37</sup> However, less attention has been paid to NK cells. Previous studies have proved that KLRG1 blockade might be a useful intervention to stimulate both NK and T cell anti-tumor immunity, which could even synergize with PD-1 checkpoint therapy.<sup>57</sup> The blockade of KLRG1 signaling in NK cells from HCV-infected individuals enhanced the production of IFN- $\gamma$  in both CD3<sup>-</sup>CD56<sup>dim</sup> and CD3<sup>-</sup>CD56<sup>bright</sup> NK cells.<sup>38</sup> Besides, *in vivo* anti-KLRG1 antibody therapy reduced lung metastases and also in combination with anti-PD-1 therapy reduced tumor volume and improved survival.<sup>58</sup> Moreover, in the context of HIV infection, the blockade of KLRG1 restored the function of a population of exhausted HIV-specific CD8<sup>+</sup> T cells, enhancing their cytokine response.<sup>59</sup> Here, we show that immunotherapy against the KLRG1 enhances NK cell function. Importantly, we detect high natural cytotoxicity and ADCC NK responses against HIV-infected targets after KLRG1 targeting, which is concordant with previous data in HCV.<sup>46</sup> In line with this result, elevated levels of E-cadherin, a ligand for the KLRG1 molecule with potential to inhibit NK cytotoxicity<sup>28</sup> and HIV-1-specific CD8<sup>+</sup> T cells, have been reported.<sup>39</sup> Thus, besides the potential benefit of targeting KLRG1 in blood, PWH could benefit from masking the interaction between KLRG1 and E-cadherin to boost their antiviral immunity in tissues.<sup>59</sup> Of relevance, we also provide direct evidence of the beneficial role of targeting KLRG1 to facilitate the elimination of the natural reservoir after *ex vivo* viral reactivation in samples from PWH.

Furthermore, we analyzed the expression of KLRG1 on CD4<sup>+</sup> T cells. We observed higher frequencies of KLRG1<sup>+</sup>CD4<sup>+</sup> T cells during untreated HIV infection, which seems to be almost normalized after ART. We believe that the elevated expression of KLRG1 on CD4<sup>+</sup> lymphocytes is the consequence of the viral-induced immune activation observed during the period of the uncontrolled infection or during HIV persistence in treated patients, rather than a direct effect of HIV on target cells. Concordantly, we observed HIV-infected cells expressing KLRG1 in the lymph nodes in VIR PWH, but we failed to observe upregulation of

KLRG1 after *ex vivo* infection of unstimulated CD4<sup>+</sup> T cells. Still, we detected proviral HIV DNA in KLRG1<sup>+</sup>CD4<sup>+</sup> T cells from ART-suppressed PWH, and targeting the KLRG1 receptor increased viral transcription. These data are in line with the idea that the expression of immune checkpoints, such as the KLRG1, on HIV reservoir cells may limit proviral expression.<sup>60</sup> Although here we do not provide information about the integrity of the reactivated viral genomes, a recent study has identified clonally expanded CD4<sup>+</sup> T cells expressing KLRG1 and harboring genome-intact HIV proviruses.<sup>60</sup>

Overall, we provide relevant information regarding the immune regulator KLRG1 during untreated and treated HIV infection in blood and tissue. Based on our results, we speculate that KLRG1 could represent a target to impact HIV persistence. Pre-clinical studies in animal models are warranted.

### Limitations of the study

The main limitations of this study are (1) the immunohistochemistry studies with lymph node samples were only performed in two PWH. We are currently making an effort to increase the repository of these precious samples. (2) We have studied the functionality of KLRG1<sup>+</sup> in blood; however, NK cells expressing this receptor might have different functional activities in different tissues.<sup>61</sup> And, (3) due to sample availability, we did not study longitudinal samples obtained from PWH. For instance, there is the possibility that very long-term ART may revert the expanded NK clusters expressing KLRG1 in PWH.

### STAR★METHODS

Detailed methods are provided in the online version of this paper and include the following:

- KEY RESOURCES TABLE
- RESOURCE AVAILABILITY
  - Lead contact
  - Materials availability
  - Data and code availability
- EXPERIMENTAL MODEL AND STUDY PARTICIPANT DETAILS
  - Human subjects
  - Cell lines
  - Plasmids
- METHOD DETAILS
  - NK cell phenotyping
  - Dimensionality reduction analysis
  - Immunohistochemistry of human lymph nodes
  - Confocal microscopy and quantification
  - NK natural cytotoxicity assay
  - *Ex vivo* infection of unstimulated PBMCs
  - NK natural cytotoxicity and ADCC against HIV<sup>+</sup> cells
  - FACS isolation of KLRG1<sup>+</sup> NK cells and CD4<sup>+</sup> T cells
  - Viral reactivation in ART-suppressed PWH samples
  - NK killing of cells harboring intact provirus
  - Intact proviral DNA assay (IPDA)
  - Quantification of HIV DNA and RNA by qPCR
- QUANTIFICATION AND STATISTICAL ANALYSIS

### SUPPLEMENTAL INFORMATION

Supplemental information can be found online at <https://doi.org/10.1016/j.xcrm.2023.101202>.

### ACKNOWLEDGMENTS

The project leading to these results has received funding from “la Caixa” Banking Foundation under the project code LCF/PR/HR20-00218. This study was also supported by the Agencia Estatal de Investigación project PID2021-123321OB-I00 funded by MCIN/AEI/10.13039/501100011033/FEDER, UE; The Spanish “Ministerio de Economía y Competitividad, Instituto de Salud Carlos III” (ISCIII, PI20/00160); and the Gilead fellowships GLD19/00084, GLD18/00008, GLD21-00049, and GLD22/00152. Part of the methodology was developed with the support of the grant 202104-30-31 from Fundació la Marató de TV3. M.B. is supported by the Miguel Servet program funded by the Spanish Health Institute Carlos III (CPII22/00005). A.A.-G. was supported by the Spanish Secretariat of Science and Innovation Ph.D. fellowship (BES-2016-076382). D.P. was supported by the VHIR Ph.D programme 2020. Spanish Secretariat of Science and Innovation Ph.D. fellowship. E.M.G. was supported by the Ramón y Cajal Program (RYC2018-024374-I) funded by the Spanish Secretariat of Science and Innovation, by the Comunidad de Madrid Talento Program (2017-T1/BMD-5396), and by the project PID2021-127899OB-I00 funded by MCIN /AEI /10.13039/501100011033/ FEDER, UE. We thank Dr. Joan Puñet from the flow cytometry core at the Vall d’Hebron Research Institute for his technical and scientific expertise. The funders had no role in study design, data collection, and analysis, the decision to publish, or preparation of the manuscript.

### AUTHOR CONTRIBUTIONS

Conceptualization, A.A.-G., D.P., and M.J.B.; methodology, A.A.-G., D.P., N.S.-G., M.C.-M., M.G., E.M.-G., and M.J.B.; investigation, A.A.-G., D.P., N.S.-G., M.C.-M., A.G.-C., J.G.-E., I.S.-C., J.R., J.C., A.C., J.B., J.N., P.S., and V.F.; resources, J.R., J.C., A.C., J.B., J.N., P.S., and V.F.; visualization, A.A.-G., D.P., and N.S.-G.; supervision, M.J.B.; funding acquisition, M.G., E.M.-G., and M.J.B.; writing – original draft, A.A.-G. and M.J.B.; writing – review & editing, A.A.-G., D.P., N.S.-G., M.C.-M., A.G.-C., J.G.-E., I.S.-C., J.R., J.C., A.C., J.B., J.N., P.S., V.F., M.G., E.M.-G., and M.J.B.

### DECLARATION OF INTERESTS

The authors declare no competing interest.

### INCLUSION AND DIVERSITY

We worked to ensure gender balance in the recruitment of human subjects. We worked to ensure ethnic or other types of diversity in the recruitment of human subjects. One or more of the authors of this paper self-identifies as a gender minority in their field of research. One or more of the authors of this paper self-identifies as a member of the LGBTQIA+ community.

Received: February 8, 2023

Revised: May 25, 2023

Accepted: August 29, 2023

Published: September 22, 2023

### REFERENCES

1. Perelson, A.S., Essunger, P., Cao, Y., Vesanen, M., Hurley, A., Saksela, K., Markowitz, M., and Ho, D.D. (1997). Decay characteristics of HIV-1-infected compartments during combination therapy. *Nature* 387, 188–191. <https://doi.org/10.1038/387188a0>.
2. Eisele, E., and Siliciano, R.F. (2012). Redefining the viral reservoirs that prevent HIV-1 eradication. *Immunity* 37, 377–388. <https://doi.org/10.1016/j.immuni.2012.08.010>.

3. Astorga-Gamaza, A., and Buzon, M.J. (2021). The active human immunodeficiency virus reservoir during antiretroviral therapy: emerging players in viral persistence. *Curr. Opin. HIV AIDS* 16, 193–199. <https://doi.org/10.1097/COH.0000000000000685>.
4. Lichtfuss, G.F., Cheng, W.J., Farsakoglu, Y., Paukovics, G., Rajasuriar, R., Velayudham, P., Kramski, M., Hearps, A.C., Cameron, P.U., Lewin, S.R., et al. (2012). Virologically suppressed HIV patients show activation of NK cells and persistent innate immune activation. *J. Immunol.* 189, 1491–1499. <https://doi.org/10.4049/jimmunol.1200458>.
5. Fenwick, C., Joo, V., Jacquier, P., Noto, A., Banga, R., Perreau, M., and Pantaleo, G. (2019). T-cell exhaustion in HIV infection. *Immunol. Rev.* 292, 149–163. <https://doi.org/10.1111/immr.12823>.
6. Nabatanzi, R., Bayigga, L., Cose, S., Rowland-Jones, S., Canderan, G., Joloba, M., and Nakanjako, D. (2019). Aberrant natural killer (NK) cell activation and dysfunction among ART-treated HIV-infected adults in an African cohort. *Clin. Immunol.* 201, 55–60. <https://doi.org/10.1016/j.clim.2019.02.010>.
7. Nabatanzi, R., Cose, S., Joloba, M., Jones, S.R., and Nakanjako, D. (2018). Effects of HIV infection and ART on phenotype and function of circulating monocytes, natural killer, and innate lymphoid cells. *AIDS Res. Ther.* 15, 7. <https://doi.org/10.1186/s12981-018-0194-y>.
8. Vivier, E., Tomasello, E., Baratin, M., Walzer, T., and Ugolini, S. (2008). Functions of natural killer cells. *Nat. Immunol.* 9, 503–510. <https://doi.org/10.1038/ni1582>.
9. Paust, S., Blish, C.A., and Reeves, R.K. (2017). Redefining Memory: Building the Case for Adaptive NK Cells. *J. Virol.* 91, e00169–17. <https://doi.org/10.1128/JVI.00169-17>.
10. Nikzad, R., Angelo, L.S., Aviles-Padilla, K., Le, D.T., Singh, V.K., Bimler, L., Vukmanovic-Stejic, M., Vendrame, E., Ranganath, T., Simpson, L., et al. (2019). Human natural killer cells mediate adaptive immunity to viral antigens. *Sci. Immunol.* 4, eaat8116. <https://doi.org/10.1126/sciimmunol.aat8116>.
11. Kim, Y., Anderson, J.L., and Lewin, S.R. (2018). Getting the "Kill" into "Shock and Kill": Strategies to Eliminate Latent HIV. *Cell Host Microbe* 23, 14–26. <https://doi.org/10.1016/j.chom.2017.12.004>.
12. Kim, J.T., Zhang, T.H., Carmona, C., Lee, B., Seet, C.S., Kostelny, M., Shah, N., Chen, H., Farrell, K., Soliman, M.S.A., et al. (2022). Latency reversal plus natural killer cells diminish HIV reservoir in vivo. *Nat. Commun.* 13, 121. <https://doi.org/10.1038/s41467-021-27647-0>.
13. Olesen, R., Vigano, S., Rasmussen, T.A., Søgaard, O.S., Ouyang, Z., Buzon, M., Bashirova, A., Carrington, M., Palmer, S., Brinkmann, C.R., et al. (2015). Innate Immune Activity Correlates with CD4 T Cell-Associated HIV-1 DNA Decline during Latency-Reversing Treatment with Panobinostat. *J. Virol.* 89, 10176–10189. <https://doi.org/10.1128/JVI.01484-15>.
14. Lanier, L.L. (2008). Up on the tightrope: natural killer cell activation and inhibition. *Nat. Immunol.* 9, 495–502. <https://doi.org/10.1038/ni1581>.
15. Horowitz, A., Strauss-Albee, D.M., Leipold, M., Kubo, J., Nemat-Gorgani, N., Dogan, O.C., Dekker, C.L., Mackey, S., Maecker, H., Swan, G.E., et al. (2013). Genetic and environmental determinants of human NK cell diversity revealed by mass cytometry. *Sci. Transl. Med.* 5, 208ra145. <https://doi.org/10.1126/scitranslmed.3006702>.
16. Hanke, T., Corral, L., Vance, R.E., and Raulet, D.H. (1998). 2F1 antigen, the mouse homolog of the rat "mast cell function-associated antigen", is a lectin-like type II transmembrane receptor expressed by natural killer cells. *Eur. J. Immunol.* 28, 4409–4417. [https://doi.org/10.1002/\(SICI\)1521-4141\(199812\)28:12<4409::AID-IMMU4409-3.0.CO;2-3](https://doi.org/10.1002/(SICI)1521-4141(199812)28:12<4409::AID-IMMU4409-3.0.CO;2-3).
17. Blaser, C., Kaufmann, M., and Pircher, H. (1998). Virus-activated CD8 T cells and lymphokine-activated NK cells express the mast cell function-associated antigen, an inhibitory C-type lectin. *J. Immunol.* 161, 6451–6454.
18. Robbins, S.H., Terrizzi, S.C., Sydora, B.C., Mikayama, T., and Brossay, L. (2003). Differential regulation of killer cell lectin-like receptor G1 expression on T cells. *J. Immunol.* 170, 5876–5885. <https://doi.org/10.4049/jimmunol.170.12.5876>.
19. Beyersdorf, N., Ding, X., Tietze, J.K., and Hanke, T. (2007). Characterization of mouse CD4 T cell subsets defined by expression of KLRG1. *Eur. J. Immunol.* 37, 3445–3454. <https://doi.org/10.1002/eji.200737126>.
20. Stephens, G.L., Andersson, J., and Shevach, E.M. (2007). Distinct subsets of FoxP3+ regulatory T cells participate in the control of immune responses. *J. Immunol.* 178, 6901–6911. <https://doi.org/10.4049/jimmunol.178.11.6901>.
21. Voehringer, D., Koschella, M., and Pircher, H. (2002). Lack of proliferative capacity of human effector and memory T cells expressing killer cell lectin-like receptor G1 (KLRG1). *Blood* 100, 3698–3702. <https://doi.org/10.1182/blood-2002-02-0657>.
22. Voehringer, D., Blaser, C., Brawand, P., Raulet, D.H., Hanke, T., and Pircher, H. (2001). Viral infections induce abundant numbers of senescent CD8 T cells. *J. Immunol.* 167, 4838–4843. <https://doi.org/10.4049/jimmunol.167.9.4838>.
23. Thimme, R., Appay, V., Koschella, M., Panther, E., Roth, E., Hislop, A.D., Rickinson, A.B., Rowland-Jones, S.L., Blum, H.E., and Pircher, H. (2005). Increased expression of the NK cell receptor KLRG1 by virus-specific CD8 T cells during persistent antigen stimulation. *J. Virol.* 79, 12112–12116. <https://doi.org/10.1128/JVI.79.18.12112-12116.2005>.
24. Ibegbu, C.C., Xu, Y.X., Harris, W., Maggio, D., Miller, J.D., and Kourtis, A.P. (2005). Expression of killer cell lectin-like receptor G1 on antigen-specific human CD8+ T lymphocytes during active, latent, and resolved infection and its relation with CD57. *J. Immunol.* 174, 6088–6094. <https://doi.org/10.4049/jimmunol.174.10.6088>.
25. Huntington, N.D., Tabarias, H., Fairfax, K., Brady, J., Hayakawa, Y., Degli-Esposti, M.A., Smyth, M.J., Tarlinton, D.M., and Nutt, S.L. (2007). NK cell maturation and peripheral homeostasis is associated with KLRG1 up-regulation. *J. Immunol.* 178, 4764–4770. <https://doi.org/10.4049/jimmunol.178.8.4764>.
26. Robbins, S.H., Nguyen, K.B., Takahashi, N., Mikayama, T., Biron, C.A., and Brossay, L. (2002). Cutting edge: inhibitory functions of the killer cell lectin-like receptor G1 molecule during the activation of mouse NK cells. *J. Immunol.* 168, 2585–2589. <https://doi.org/10.4049/jimmunol.168.6.2585>.
27. Tessmer, M.S., Fugere, C., Stevenaert, F., Naidenko, O.V., Chong, H.J., Leclercq, G., and Brossay, L. (2007). KLRG1 binds cadherins and preferentially associates with SHIP-1. *Int. Immunol.* 19, 391–400. <https://doi.org/10.1093/intimm/dxm004>.
28. Ito, M., Maruyama, T., Saito, N., Koganei, S., Yamamoto, K., and Matsu-moto, N. (2006). Killer cell lectin-like receptor G1 binds three members of the classical cadherin family to inhibit NK cell cytotoxicity. *J. Exp. Med.* 203, 289–295. <https://doi.org/10.1084/jem.20051986>.
29. Müller-Durovic, B., Lanna, A., Covre, L.P., Mills, R.S., Henson, S.M., and Akbar, A.N. (2016). Killer Cell Lectin-like Receptor G1 Inhibits NK Cell Function through Activation of Adenosine 5'-Monophosphate-Activated Protein Kinase. *J. Immunol.* 197, 2891–2899. <https://doi.org/10.4049/jimmunol.1600590>.
30. Gründemann, C., Bauer, M., Schweier, O., von Oppen, N., Lässig, U., Saudan, P., Becker, K.F., Karp, K., Hanke, T., Bachmann, M.F., and Pircher, H. (2006). Cutting edge: identification of E-cadherin as a ligand for the murine killer cell lectin-like receptor G1. *J. Immunol.* 176, 1311–1315. <https://doi.org/10.4049/jimmunol.176.3.1311>.
31. Li, Y., Hofmann, M., Wang, Q., Teng, L., Chlewicki, L.K., Pircher, H., and Mariuzza, R.A. (2009). Structure of natural killer cell receptor KLRG1 bound to E-cadherin reveals basis for MHC-independent missing self recognition. *Immunity* 31, 35–46. <https://doi.org/10.1016/j.immuni.2009.04.019>.
32. Banga, R., Procopio, F.A., Noto, A., Pollakis, G., Cavassini, M., Ohmiti, K., Corpataux, J.M., de Leval, L., Pantaleo, G., and Perreau, M. (2016). PD-1(+) and follicular helper T cells are responsible for persistent HIV-1

- transcription in treated aviremic individuals. *Nat. Med.* 22, 754–761. <https://doi.org/10.1038/nm.4113>.
33. Serra-Peinado, C., Grau-Expósito, J., Luque-Ballesteros, L., Astorga-Gamaza, A., Navarro, J., Gallego-Rodríguez, J., Martín, M., Curran, A., Burgos, J., Ribera, E., et al. (2019). Expression of CD20 after viral reactivation renders HIV-reservoir cells susceptible to Rituximab. *Nat. Commun.* 10, 3705. <https://doi.org/10.1038/s41467-019-11556-4>.
  34. Guo, A.L., Jiao, Y.M., Zhao, Q.W., Huang, H.H., Deng, J.N., Zhang, C., Fan, X., Xu, R.N., Zhang, J.Y., Zhen, C., et al. (2022). Implications of the accumulation of CXCR5(+) NK cells in lymph nodes of HIV-1 infected patients. *EBioMedicine* 75, 103794. <https://doi.org/10.1016/j.ebiom.2021.103794>.
  35. Huot, N., Jacquelin, B., Garcia-Tellez, T., Rasclé, P., Ploquin, M.J., Madec, Y., Reeves, R.K., Derreudre-Bosquet, N., and Müller-Trutwin, M. (2017). Natural killer cells migrate into and control simian immunodeficiency virus replication in lymph node follicles in African green monkeys. *Nat. Med.* 23, 1277–1286. <https://doi.org/10.1038/nm.4421>.
  36. Groom, J.R., and Luster, A.D. (2011). CXCR3 ligands: redundant, collaborative and antagonistic functions. *Immunol. Cell Biol.* 89, 207–215. <https://doi.org/10.1038/icb.2010.158>.
  37. Wei, S.C., Duffy, C.R., and Allison, J.P. (2018). Fundamental Mechanisms of Immune Checkpoint Blockade Therapy. *Cancer Discov.* 8, 1069–1086. <https://doi.org/10.1158/2159-8290.CD-18-0367>.
  38. Wang, J.M., Cheng, Y.Q., Shi, L., Ying, R.S., Wu, X.Y., Li, G.Y., Moorman, J.P., and Yao, Z.Q. (2013). KLRG1 negatively regulates natural killer cell functions through the Akt pathway in individuals with chronic hepatitis C virus infection. *J. Virol.* 87, 11626–11636. <https://doi.org/10.1128/JVI.01515-13>.
  39. Streeck, H., Kwon, D.S., Pyo, A., Flanders, M., Chevalier, M.F., Law, K., Jülg, B., Trocha, K., Jolin, J.S., Anahar, M.N., et al. (2011). Epithelial adhesion molecules can inhibit HIV-1-specific CD8(+) T-cell functions. *Blood* 117, 5112–5122. <https://doi.org/10.1182/blood-2010-12-321588>.
  40. Astorga-Gamaza, A., Grau-Expósito, J., Burgos, J., Navarro, J., Curran, A., Planas, B., Suanzes, P., Falcó, V., Genescà, M., and Buzon, M.J. (2022). Identification of HIV-reservoir cells with reduced susceptibility to antibody-dependent immune response. *Elife* 11, e78294. <https://doi.org/10.7554/eLife.78294>.
  41. Fromentin, R., DaFonseca, S., Costiniuk, C.T., El-Far, M., Procopio, F.A., Hecht, F.M., Hoh, R., Deeks, S.G., Hazuda, D.J., Lewin, S.R., et al. (2019). PD-1 blockade potentiates HIV latency reversal ex vivo in CD4(+) T cells from ART-suppressed individuals. *Nat. Commun.* 10, 814. <https://doi.org/10.1038/s41467-019-08798-7>.
  42. Lian, X., Seiger, K.W., Parsons, E.M., Gao, C., Sun, W., Gladkov, G.T., Roseto, I.C., Einkauf, K.B., Osborn, M.R., Chevalier, J.M., et al. (2023). Progressive transformation of the HIV-1 reservoir cell profile over two decades of antiviral therapy. *Cell Host Microbe* 31, 83–96.e5. <https://doi.org/10.1016/j.chom.2022.12.002>.
  43. Duette, G., Hiener, B., Morgan, H., Mazur, F.G., Mathivanan, V., Horsburgh, B.A., Fisher, K., Tong, O., Lee, E., Ahn, H., et al. (2022). The HIV-1 proviral landscape reveals that Nef contributes to HIV-1 persistence in effector memory CD4+ T cells. *J. Clin. Invest.* 132, e154422. <https://doi.org/10.1172/JCI154422>.
  44. Ren, Y., Huang, S.H., Patel, S., Alberto, W.D.C., Magat, D., Ahimovic, D., Macedo, A.B., Durga, R., Chan, D., Zale, E., et al. (2020). BCL-2 antagonism sensitizes cytotoxic T cell-resistant HIV reservoirs to elimination ex vivo. *J. Clin. Invest.* 130, 2542–2559. <https://doi.org/10.1172/JCI132374>.
  45. Pino, M., Pagliuzza, A., Pampena, M.B., Deleage, C., Viox, E.G., Nguyen, K., Shim, I., Zhang, A., Harper, J.L., Samer, S., et al. (2022). Limited impact of fingolimod treatment during the initial weeks of ART in SIV-infected rhesus macaques. *Nat. Commun.* 13, 5055. <https://doi.org/10.1038/s41467-022-32698-y>.
  46. Wijaya, R.S., Read, S.A., Schibeci, S., Eslam, M., Azardaryany, M.K., El-Khobar, K., van der Poorten, D., Lin, R., Yuen, L., Lam, V., et al. (2019). KLRG1+ natural killer cells exert a novel antifibrotic function in chronic hepatitis B. *J. Hepatol.* 71, 252–264. <https://doi.org/10.1016/j.jhep.2019.03.012>.
  47. Borys, S.M., Bag, A.K., Brossay, L., and Adeegbe, D.O. (2022). The Yin and Yang of Targeting KLRG1(+) Tregs and Effector Cells. *Front. Immunol.* 13, 894508. <https://doi.org/10.3389/fimmu.2022.894508>.
  48. Novelli, L., Barbati, C., Capuano, C., Recalchi, S., Ceccarelli, F., Vomero, M., Alessandri, C., Morrone, S., and Conti, F. (2023). KLRG1 is reduced on NK cells in SLE patients, inversely correlates with disease activity and is modulated by hydroxychloroquine in vitro. *Lupus* 32, 549–559. <https://doi.org/10.1177/09612033231160979>.
  49. Moretta, L. (2010). Dissecting CD56dim human NK cells. *Blood* 116, 3689–3691. <https://doi.org/10.1182/blood-2010-09-303057>.
  50. Nie, Y., Liu, D., Yang, W., Li, Y., Zhang, L., Cheng, X., Chen, R., Yuan, B., Zhang, G., and Wang, H. (2022). Increased expression of TIGIT and KLRG1 correlates with impaired CD56(bright) NK cell immunity in HPV16-related cervical intraepithelial neoplasia. *Viol. J.* 19, 68. <https://doi.org/10.1186/s12985-022-01776-4>.
  51. Alpert, M.D., Harvey, J.D., Lauer, W.A., Reeves, R.K., Piatak, M., Jr., Carville, A., Mansfield, K.G., Lifson, J.D., Li, W., Desrosiers, R.C., et al. (2012). ADCC develops over time during persistent infection with live-attenuated SIV and is associated with complete protection against SIV(mac)251 challenge. *PLoS Pathog.* 8, e1002890. <https://doi.org/10.1371/journal.ppat.1002890>.
  52. Haynes, B.F., Gilbert, P.B., McElrath, M.J., Zolla-Pazner, S., Tomaras, G.D., Alam, S.M., Evans, D.T., Montefiori, D.C., Karnasuta, C., Sutthent, R., et al. (2012). Immune-correlates analysis of an HIV-1 vaccine efficacy trial. *N. Engl. J. Med.* 366, 1275–1286. <https://doi.org/10.1056/NEJMoa1113425>.
  53. Lopez-Vergès, S., Milush, J.M., Schwartz, B.S., Pando, M.J., Jarjoura, J., York, V.A., Houchins, J.P., Miller, S., Kang, S.M., Norris, P.J., et al. (2011). Expansion of a unique CD57(+)NKG2Chi natural killer cell subset during acute human cytomegalovirus infection. *Proc. Natl. Acad. Sci. USA* 108, 14725–14732. <https://doi.org/10.1073/pnas.1110900108>.
  54. Wijaya, R.S., Read, S.A., Selvamani, S.P., Schibeci, S., Azardaryany, M.K., Ong, A., van der Poorten, D., Lin, R., Douglas, M.W., George, J., and Ahlenstiel, G. (2021). Hepatitis C Virus (HCV) Eradication With Interferon-Free Direct-Acting Antiviral-Based Therapy Results in KLRG1+ HCV-Specific Memory Natural Killer Cells. *J. Infect. Dis.* 223, 1183–1195. <https://doi.org/10.1093/infdis/jiaa492>.
  55. Judge, S.J., Murphy, W.J., and Canter, R.J. (2020). Characterizing the Dysfunctional NK Cell: Assessing the Clinical Relevance of Exhaustion, Anergy, and Senescence. *Front. Cell. Infect. Microbiol.* 10, 49. <https://doi.org/10.3389/fcimb.2020.00049>.
  56. Alvarez, M., Simonetta, F., Baker, J., Pierini, A., Wenokur, A.S., Morrison, A.R., Murphy, W.J., and Negrin, R.S. (2019). Regulation of murine NK cell exhaustion through the activation of the DNA damage repair pathway. *JCI Insight* 5, e127729. <https://doi.org/10.1172/jci.insight.127729>.
  57. Tata, A., Dodard, G., Fugère, C., Leget, C., Ors, M., Rossi, B., Vivier, E., and Brossay, L. (2021). Combination blockade of KLRG1 and PD-1 promotes immune control of local and disseminated cancers. *Onc Immunology* 10, 1933808. <https://doi.org/10.1080/2162402X.2021.1933808>.
  58. Greenberg, S.A., Kong, S.W., Thompson, E., and Gulla, S.V. (2019). Co-inhibitory T cell receptor KLRG1: human cancer expression and efficacy of neutralization in murine cancer models. *Oncotarget* 10, 1399–1406. <https://doi.org/10.18632/oncotarget.26659>.
  59. Wang, S., Zhang, Q., Hui, H., Agrawal, K., Karris, M.A.Y., and Rana, T.M. (2020). An atlas of immune cell exhaustion in HIV-infected individuals revealed by single-cell transcriptomics. *Emerg. Microb. Infect.* 9, 2333–2347. <https://doi.org/10.1080/22221751.2020.1826361>.

60. Sun, W., Gao, C., Hartana, C.A., Osborn, M.R., Einkauf, K.B., Lian, X., Bone, B., Bonheur, N., Chun, T.W., Rosenberg, E.S., et al. (2023). Phenotypic signatures of immune selection in HIV-1 reservoir cells. *Nature* 614, 309–317. <https://doi.org/10.1038/s41586-022-05538-8>.
61. Dogra, P., Rancan, C., Ma, W., Toth, M., Senda, T., Carpenter, D.J., Kubota, M., Matsumoto, R., Thapa, P., Szabo, P.A., et al. (2020). Tissue Determinants of Human NK Cell Development, Function, and Residence. *Cell* 180, 749–763.e13. <https://doi.org/10.1016/j.cell.2020.01.022>.
62. Bruner, K.M., Wang, Z., Simonetti, F.R., Bender, A.M., Kwon, K.J., Sengupta, S., Fray, E.J., Beg, S.A., Antar, A.A.R., Jenike, K.M., et al. (2019). A quantitative approach for measuring the reservoir of latent HIV-1 proviruses. *Nature* 566, 120–125. <https://doi.org/10.1038/s41586-019-0898-8>.

STAR★METHODS

KEY RESOURCES TABLE

REAGENT or RESOURCE	SOURCE	IDENTIFIER
<b>Antibodies</b>		
Brilliant Violet 650 anti-human CD183 (CXCR3) Clone G025H7	Biologend	Cat#353730; RRID:AB_2563870
PerCP-Cy5.5 anti-human CD57 Clone HNK-1	Biologend	Cat#359622; RRID:AB_2565930
FITC anti-human CD56 Clone B159	Becton Dickinson	Cat#562794; RRID:AB_2737799
PE-Cy7 anti-Human CD3 Clone SK7	Becton Dickinson	Cat#557851; RRID:AB_396896
PerCP anti-human CD3 Clone SK7	Becton Dickinson	Cat#347344; RRID:AB_400286
APC anti-human CD3 Clone SK7	Biologend	Cat#344811; RRID:AB_10644010
PE-Dazzle 594 anti-human CD337 (NKp30) Clone P30-15	Biologend	Cat#325231; RRID:AB_2814184
PE anti-human NKG2C Clone 134591	R&D Systems	Cat#FAB138P-100
APC-Cy7 anti-human NKG2D Clone 1D11	Biologend	Cat#320823; RRID:AB_2566659
AF700 anti-Human CD4 Clone RPA-T4	Becton Dickinson	Cat#557922; RRID:AB_396943
BV605 anti-human CD4 Clone RPA-T4	Becton Dickinson	Cat#562658; RRID:AB_2744420
V500 anti-human CD8 Clone RPA-T8	Becton Dickinson	Cat#560774; RRID:AB_1937325
APC anti-human CD8 Clone RPA-T8	Becton Dickinson	Cat#555369; RRID:AB_398595
APC anti-human CD159a (NKG2A) Clone Z199	Beckman Coulter	Cat#A60797; RRID:AB_10643105
BV786 anti-human CD16 Clone 3G8	Becton Dickinson	Cat#563690
BV605 anti-human CD158b (KIR2DL2/L3/S2) Clone CH-L	Becton Dickinson	Cat#743453; RRID:AB_2741518
BV421 anti-human KLRG1 Clone 14C2A07	Biologend	Cat#368604; RRID:AB_2566593
PE-Cy5 anti-human CD107a Clone H4A3	Becton Dickinson	Cat#555802; RRID:AB_396136
AF700 anti-human IFN- $\gamma$ Clone B27	Invitrogen	Cat#MHCIFG29; RRID:AB_2539767
APC-Fire750 anti-human CD19 Clone HIB19	Biologend	Cat#302258; RRID:AB_2629691
PE-CF594 anti-human CD69 Clone FN50	Becton Dickinson	Cat#562617; RRID:AB_2737680
SB600 anti-human HLA-DR Clone LN3	Invitrogen	Cat#63-9956-42; RRID:AB_2637402
PE-CF594 anti-human E-cadherin Clone 67A4	Becton Dickinson	Cat#563572; RRID:AB_2738284
Purified anti-mouse/human E-cadherin Clone DECMA-1	Biologend	Cat#147301; RRID:AB_2563037
PE mouse anti-p24 Clone KC57	Beckman Coulter	Cat#6604667; RRID:AB_1575989
Mouse anti-human p24 Clone Kal-1	Dako-Agilent	Cat#M0857 Discontinued
Rabbit-polyclonal anti-human KLRG1	Abcam	Cat#ab235951
Goat-polyclonal anti-human CD56	R&D Systems	Cat#AF2408; RRID:AB_442152
AF568 donkey-polyclonal anti-goat IgG	Invitrogen	Cat#A-11057; RRID:AB_142581
AF647 donkey-polyclonal anti-mouse IgG	Invitrogen	Cat#A-31571; RRID:AB_162542
AF488 donkey-polyclonal anti-rabbit IgG	Invitrogen	Cat#A-21206; RRID:AB_2535792
Purified Mouse IgG2a, $\kappa$ Isotype Ctrl Clone MOPC-173	Biologend	Cat#400201
Purified Rat IgG1, $\kappa$ Isotype Ctrl Clone RTK2071	Biologend	Cat#400401; RRID:AB_326507
Human Fc Block Clone Fc1	Becton Dickinson	Cat#564219; RRID:AB_2728082
<b>Bacterial and virus strains</b>		
Plasmid encoding HIV-1 strain NL4.3	NIH AIDS Reagent Program	Cat#2006
HIV-1 Ba-L	HIV Reagent Program	Cat#ARP-510
<b>Biological samples</b>		
Human peripheral blood mononuclear cells (PBMCs) from people with HIV (PWH)	HIV unit Hospital Universitari Vall d'Hebron (Barcelona)	This paper
PBMCs from uninfected donors	Blood and Tissue Bank (Barcelona)	This paper
Tissue sections from human lymph nodes of HIV-infected PWH	Anatomical Pathology Department of the Hospital Universitari Vall d'Hebron (Barcelona)	This paper

(Continued on next page)

REAGENT or RESOURCE	SOURCE	IDENTIFIER
<b>Continued</b>		
<b>Chemicals, peptides, and recombinant proteins</b>		
Ionomycin	Abcam	Cat#ab120370
Phorbol 12-myristate 13-acetate	Abcam	Cat#ab120297
Romidepsin	Selleckchem	Cat#S3020
Raltegravir	NIH AIDS Reagent Program	Cat#0980
Darunavir	NIH AIDS Reagent Program	Cat#0989
Nevirapine	Sigma Aldrich	Cat#SML0097-10MG
Q-VD-OPh (quinolyl-valyl-O-methylaspartyl- [-2,6-difluorophenoxy]-methyl ketone	Selleckchem	Cat#S7311
SuperScript III Reverse Transcriptase	Invitrogen	Cat#18080044
Proteinase K from <i>Tritirachium album</i>	Sigma Aldrich	Cat#P4850
Human IL-2	Sigma Aldrich	Cat#11011456001
Human IL-15	Miltenyi Biotec	Cat#130-093-955
Recombinant human E-cadherin	R&D Systems	Cat#8505-EC-050
BD GolgiPlug Protein Transport Inhibitor (Containing Brefeldin A)	Becton Dickinson	Cat#555029
BD GolgiStop Protein Transport Inhibitor (Containing Monensin)	Becton Dickinson	Cat#554724
DAPI (4',6-diamidino-2-phenylindole-dilactate)	Invitrogen	Cat#D3571
Fluoromount G	Invitrogen	Cat#00-4958-02
<b>Critical commercial assays</b>		
MagniSort Human NK cell Enrichment Kit	Invitrogen	Cat#8804-6819-74
MagniSort Human CD4 <sup>+</sup> T cell Enrichment Kit	Invitrogen	Cat#8804-6811-74
Dynabeads CD4 Positive Isolation Kit	Invitrogen	Cat#11331D
EasySep Dead Cell Removal (Annexin V) Kit	StemCell	Cat#17899
RNeasy Plus Micro Kit	Qiagen	Cat#74034
NZY Total RNA Kit	NZYtech	Cat#MB13402
BD Cytotfix/Cytoperm Fixation/Permeabilization Kit	Becton Dickinson	Cat#554714
BD Horizon Brilliant Stain Buffer	Becton Dickinson	Cat#566349
LIVE/DEAD Fixable Aqua Dead Cell Stain Kit	Invitrogen	Cat#L34966
LIVE/DEAD Fixable Far Red Dead Cell Stain Kit	Invitrogen	Cat#L34974
<b>Experimental models: Cell lines</b>		
K562 human myelogenous leukemia cell line	Sigma Aldrich	Cat#89121407
<b>Oligonucleotides</b>		
HIV-1 $\Psi$ forward primer: 5'-CAGGACTCGGCTTGCTGAAG-3'	IDT	N/A
HIV-1 $\Psi$ reverse primer: 5'-GCACCCATCTCTCCTTCTAGC-3'	IDT	N/A
HIV-1 $\Psi$ probe: 5'-6-FAM-TTTTGGCGTACTCACCAGT-MGBNFQ-3'	ThermoFisher Scientific	N/A
HIV-1 <i>env</i> forward primer: 5'-AGTGGTGCAGAGAGAAAAAGAGC-3'	IDT	N/A
HIV-1 <i>env</i> reverse primer: 5'-GTCTGGCCTGTACCGTCAGC-3'	IDT	N/A
HIV-1 <i>env</i> probe: 5'-VIC-CCTTGGGTTCTTGGGA-MGBNFQ-3'	ThermoFisher Scientific	N/A
HIV-1 anti-Hypermutant <i>env</i> probe: 5'-CCTTAGGTTCTTAGGAGC-MGBNFQ-3'	ThermoFisher Scientific	N/A
<i>hRPP30</i> forward primer: 5'-GATTGGACCTGCGAGCG-3'	IDT	N/A

(Continued on next page)

**Continued**

REAGENT or RESOURCE	SOURCE	IDENTIFIER
<i>hRPP30</i> reverse primer: 5'-GCGGCTGTCTCCACAAGT-3'	IDT	N/A
<i>hRPP30</i> probe: 5'-6-FAM-CTGACCTGA/ZEN/AGGCTCT/3IABkFQ-3'	IDT	N/A
1-LTR HIV-1 forward primer: 5'-TTAAGCCTCAATAAAGCTTGCC-3'	IDT	N/A
1-LTR HIV-1 reverse primer: 5'-GTTCCGGCGCCACTGCTAG-3'	IDT	N/A
1-LTR HIV-1 probe: 5'-/56-FAM/CCAGAGTCA/ZEN/CACAACAGA CGGGCA/31ABkFQ/-3'	IDT	N/A
<i>CCR5</i> forward primer: 5'-GCTGTGTTTGCCTCTCTCCAGGA-3'	IDT	N/A
<i>CCR5</i> reverse primer: 5'-CTCACAGCCCTGTGCCTTCTTTC-3'	IDT	N/A
<i>CCR5</i> probe: 5'-/56-FAM/AGCAGCGGC/ZEN/AGGACCAG CCCCAAG/3IABkFQ/-3'	IDT	N/A

**Software and algorithms**

ImageJ 1.53c	National Institutes of Health, USA	<a href="https://imagej.nih.gov/ij/index.html">https://imagej.nih.gov/ij/index.html</a>
OMIQ	Dotmatics	<a href="http://www.omiq.ai">www.omiq.ai</a> , <a href="http://www.dotmatics.com">www.dotmatics.com</a>
FlowJo V10	Becton Dickinson	<a href="https://www.flowjo.com/">https://www.flowjo.com/</a>
GraphPad V8	GraphPad Software	<a href="https://www.graphpad.com/">https://www.graphpad.com/</a>
BioRender	BioRender	<a href="https://www.biorender.com/">https://www.biorender.com/</a>

**RESOURCE AVAILABILITY**

**Lead contact**

We have tried to provide as much information as possible regarding the reagents used in this study. Nonetheless, further information and requests for resources and reagents should be directed to and will be fulfilled by the lead contact, Dr. Maria J Buzón ([mariajose.buzon@vhir.org](mailto:mariajose.buzon@vhir.org)).

**Materials availability**

This study did not generate new unique reagents. All reagents used are indicated in this section and are available. All plasmids needed for the generation of viral stocks were obtained through the NIH AIDS Reagent Program.

**Data and code availability**

All data reported in this paper will be shared by the lead contact upon request. Due to the sensitivity of the data, individual participant data will not be shared. This paper does not report original code. Any additional information required to reanalyze the data reported in this paper is available from the lead contact upon request.

**EXPERIMENTAL MODEL AND STUDY PARTICIPANT DETAILS**

**Human subjects**

In this study, we used primary cells obtained from blood samples from people with HIV (PWH) and non-HIV donors. Peripheral blood mononuclear cells (PBMCs) PWH were obtained from the HIV unit of the Hospital Universitari Vall d'Hebron in Barcelona, Spain. Study protocols were approved by the corresponding Ethical Committees (Institutional Review Board numbers PR(AG)270/2015, PR(AG)192/2018, and PR(AG)476–2018). PBMCs from healthy donors were obtained from the Blood and Tissue Bank, in Barcelona, Spain. All subjects recruited for this study were adults who provided written informed consent. Samples were prospectively collected and cryopreserved in the Biobank (register number C.0003590). Information on plasma viral loads, CD4<sup>+</sup> T cell counts, and time on ART from suppressed PWH is summarized in [Table S1](#). Gender and age are also indicated for PWH in [Table S1](#); however, this information is not available for uninfected donors. Since we utilized samples from donors of different genders in our experiments, we can conclude that the strategy presented here for stimulating the elimination of HIV reservoirs by targeting the receptor KLRG1 applies to

both men and women. PBMCs were obtained by Ficoll-Paque density gradient centrifugation and cryopreserved in liquid nitrogen. PBMCs were cultured in RPMI medium (Gibco) supplemented with 10% Fetal Bovine Serum (Gibco), 100  $\mu\text{g}/\text{mL}$  streptomycin (Fisher Scientific), and 100 U/ml penicillin (Fisher Scientific) (R10 medium), and maintained at 37°C in a 5% CO<sub>2</sub> incubator, when needed. CD4<sup>+</sup> T cells and NK cells were isolated from PBMCs using commercial kits (MagneSort Human CD4<sup>+</sup> T cell Enrichment; Affymetrix, and MagneSort Human NK cell Enrichment; eBioscience). Two rounds of cell separation were performed to maximize the purity of the cells (overall purity >85%). In some experiments, CD4<sup>+</sup> T cells and NK cells were obtained by fluorescence-activated cell sorting from PBMC samples (Cytex Aurora CS). Paraffin-embedded LN samples from PWH were obtained from the Anatomical Pathology Department of the Hospital Universitari Vall d'Hebron (Barcelona, Spain). Written informed consent was provided by all participants.

### Cell lines

We also used the K-562 cell line, a widespread and highly sensitive *in vitro* target model to study the natural cytotoxicity function of natural killer cells. K562 human myelogenous leukemia cell line was obtained from the NIH AIDS Reagent Program Division of AIDS, NIAID, NIH. These cells were cultured in R10 medium and maintained at 37°C in a 5% CO<sub>2</sub> incubator. We checked the absence of contaminants in our cell cultures.

### Plasmids

All plasmids needed for the generation of viral stocks were obtained through the NIH AIDS Reagent Program. Viral stocks were generated by transfection of 293T cells with the plasmids encoding the different molecular clones, and the resulting viral particles were titrated in TZMbl cells using an enzyme luminescence assay (Britelite plus kit; PerkinElmer) as described previously. Palivizumab was obtained from the Vall d'Hebron Hospital pharmacy.

### METHOD DETAILS

In this section, detailed information about the different assays performed can be found. Information on the sample size and the number of replicates for each assay is indicated in each figure legend. Our criteria for the inclusion of different samples from PWH in the different assays was mainly related to their control status of the disease, particularly their viral load and CD4<sup>+</sup> T cell counts. The assays on viral reservoir cells presented here are complex, among other factors due to the scarcity of HIV-reservoir cells in samples. We started these assays with a large number of cells to avoid errors in the interpretations of the results. Other measures to control and assure the proper analysis of the data are detailed for each assay, such as the use of Fluorescence Minus One (FMO) controls in flow cytometry experiments or isotype antibodies in functional assays to exclude non-specific effects.

### NK cell phenotyping

PBMCs were stained with LIVE/DEAD AQUA viability (Invitrogen) for 20 min at room temperature (RT). After washing once with staining buffer (1X PBS 3% FBS), cells were stained with anti-CXCR3-BV650 (G025H7, Biolegend) for 30 min at 37°C. Next, we performed a washing step with a staining buffer and a new staining with anti-CD57-PerCP-Cy5.5 (HNK-1, Biolegend), anti-CD56-FITC (B159, Becton Dickinson), anti-CD3-PE-Cy7 (SK7, Becton Dickinson), anti-NKp30-PE-CF594 (P30-15, Biolegend), anti-NKG2C-PE (134591, R&D Systems), anti-NKG2D-APC-Cy7 (1D11, Biolegend), anti-CD4-AF700 (RPA-T4, Becton Dickinson), anti-NKG2A-APC (Z199, Beckman Coulter), anti-CD16-BV786 (3G8, Becton Dickinson), anti-CD158b-BV605 (CH-L, Becton Dickinson) and anti-KLRG1-BV421 (14C2A07, Biolegend) antibodies for 20 min at RT. Cells were then washed and fixed with 2% PFA. Samples were acquired on a BD LSR Fortessa flow cytometer and data was analyzed using FlowJo V10 software. Gating was performed according to the different FMO controls.

### Dimensionality reduction analysis

Dimensionality reduction analysis (optSNE) of flow cytometry data was performed using the OMIQ software from Dotmatics ([www.omiq.ai](http://www.omiq.ai), [www.dotmatics.com](http://www.dotmatics.com)). All events within pre-gated CD56<sup>+</sup> NK cells were concatenated for each group per culture condition and analyzed. OptSNE clustering was performed on equal samples of randomly selected 6 x 10<sup>5</sup> cells from each group based on expression of CD57, NKp30, NKG2C, NKG2D, NKG2A, CD16, CXCR3, CD158b and KLRG1, followed by Flow-Self Organizing Maps (FlowSOM) artificial intelligence algorithm for cluster identification. Marker expression was represented as Archsinh-transformed medians within heatmaps generated via optSNE analysis.

### Immunohistochemistry of human lymph nodes

For immunodetection of KLRG1, CD56, and p24, formalin-fixed and paraffin-embedded (FFPE) tissue sections from human lymph nodes of HIV-infected PWH were subjected to deparaffinization (using xylene and decreasing ethanol concentrations), hydration and heat-induced epitope retrieval with a PT-LINK (Dako). Then, the slides were permeabilized in 1X Tris-buffered saline (TBS) (Fisher Scientific) with 0.1% Triton X-100 (Sigma-Aldrich) and 1% BSA (Sigma-Aldrich) for 10 min. Subsequently, blocking was performed for 2 h with 1X TBS supplemented with 10% normal donkey serum (Jackson ImmunoResearch) and 1% BSA before staining. The slides were then incubated with the primary antibodies overnight at 4 °C: anti-CD56 (goat-polyclonal anti-CD56 antibody, 10  $\mu\text{g}/\text{mL}$ , R&D Systems clone NCAM-1), anti-KLRG1 (rabbit-polyclonal anti-KLRG1 antibody, 1/100, Abcam ab235951),

or anti-p24 (mouse-monoclonal anti-p24 antibody, 1/10, Dako-Agilent M0857), diluted in 1xTBS and 1% BSA. Next, samples were washed and incubated for 1 h at 37°C with the appropriate secondary antibodies: Alexa Fluor 568 donkey anti-goat (Invitrogen), Alexa Fluor 647 donkey anti-mouse (Invitrogen), and Alexa Fluor 488 donkey anti-rabbit (Invitrogen), counterstained with DAPI (4',6-diamidino-2-phenylindole-dilactate, ThermoFisher), and mounted with Fluoromount G (eBioscience).

### Confocal microscopy and quantification

Samples were imaged on a Leica TCS SP5 and Zeiss LSM780 confocal microscopes, using an  $\times 20$  and  $\times 40$  phase objective and sequential mode to separately capture the fluorescence from the different fluorochromes. Tiles were merged with the LAS AF software. ImageJ 1.53c software (National Institutes of Health, USA) was used to perform image processing and analysis. For CD56/KLRG1 and p24/KLRG1 co-localization analysis, a binary mask was generated for each channel, and the “analyze particles” tool and manual recount were used to count single and double-stained cells. In all experiments, at least 6 B-cell follicles were analyzed per sample.

### NK natural cytotoxicity assay

NK cytotoxicity was measured by the detection of CD107a and IFN- $\gamma$  by flow cytometry after co-culture with the K562 cells alone or in combination with IL-15. NK cells were isolated using a commercial kit (MagneSort Human NK Cell Enrichment; Affymetrix) and co-cultured with K562 in a 1:1 ratio. CD107a-PE-Cy5 (H4A3; Becton Dickinson), BD Golgiplug Protein Transport Inhibitor (Becton Dickinson), and BD GolgiStop Protein Transport Inhibitor containing monensin (Becton Dickinson) were also added to each well at the recommended concentrations. Human IL-15 (Miltenyi Biotec) was added to the corresponding wells at 25 ng/mL. Plates were centrifuged and incubated for 4.5 h at 37°C and 5% CO<sub>2</sub>. Cells were then washed and stained with a viability dye (LIVE/DEAD Fixable Aqua Dead Cell Stain; Thermo Fisher). After that, cells were stained with anti-CD57-PerCP-Cy5.5 (HNK-1; Biolegend), anti-CD56-FITC (B159; Becton Dickinson), anti-CD3-PE-Cy7 (SK7; Becton Dickinson), anti-CD69-PE-CF594 (FN50; Becton Dickinson), anti-NKG2C-PE (134591; R&D systems), anti-CD16-BV786 (3G8; Becton Dickinson) and anti-HLA-DR-SB600 (LN3; eBioscience) antibodies for 20 min at RT. Cells were then fixed and permeabilized with Fixation/Permeabilization Solution (Becton Dickinson) for 20 min at 4°C, washed with BD Perm/Wash buffer and stained with anti-IFN- $\gamma$ -AF700 (B27; Life Technologies) for 30 min at RT. After washing, cells were fixed with PFA (2%) and acquired on an LSR Fortessa flow cytometer (Becton Dickinson). Data were analyzed using FlowJo V10 software.

### Ex vivo infection of unstimulated PBMCs

PBMCs from ART-suppressed PWH were thawed and incubated overnight in R10 medium containing 40 U/ml of IL-2. The next day, CD4<sup>+</sup> T cells were isolated using a commercial kit (MagneSort Human CD4<sup>+</sup> T cell Enrichment; Affymetrix) and infected by spinoculation at 1200xg for 2 h at 37°C with HIV<sub>NL4.3</sub> or HIV<sub>BaL</sub> viral strains (50% tissue culture infectious dose (TCID<sub>50</sub>) of 78,125 and 625 for HIV<sub>NL4.3</sub> and HIV<sub>BaL</sub>, respectively). Cells were then washed twice with PBS and cultured at 1 million/ml in a 96-well plate round-bottom with R10 containing 100 U/ml of IL-2 for the next 5 days. The resulting HIV-infected CD4<sup>+</sup> T cells were used for different experiments listed below.

### NK natural cytotoxicity and ADCC against HIV<sup>+</sup> cells

Five days after HIV infection, cells were placed in 96-well plates round-bottom at 100,000 cells/well. Autologous NK cells, previously isolated by negative selection using magnetic beads (MagneSort Human NK cell Enrichment Kit, eBioscience) from PBMCs, were then added at a 1:1 ratio. Two rounds of cell separation were performed to maximize the purity of the cells (overall purity >85%). In some experiments, we assessed the effect of targeting KLRG1 with antibodies. In such cases, NK cells were previously incubated with the anti-KLRG1 monoclonal antibody (6  $\mu$ g/mL clone 14C2A07, Biolegend) for 20 min and then washed with staining buffer to remove the unbound antibodies before the co-culture. As a control, we also included NK cells cultured with the isotype mouse IgG2a k (6  $\mu$ g/mL) (MOPC-173, Biolegend). Additionally, a pool of NK cells previously treated with an Fc receptor blocker (human Fc block, Becton Dickinson) and then incubated with the anti-KLRG1 antibody was used as a control. Plates were then centrifuged at 400g for 3 min and incubated for 4 h at 37°C and 5% CO<sub>2</sub>. For the ADCC assays, HIV-infected CD4<sup>+</sup> T cells were incubated for 15 min with plasma (1:1,000 dilution) from a VIR HIV<sup>+</sup> PWH containing a mix of antibodies targeting different HIV epitopes, before the 4 h co-culture with the NK cells. After incubation, cells were transferred to a V-bottom 96 well plate, washed with PBS, and stained with a viability dye (LIVE/DEAD Fixable Aqua Dead Cell Stain; Thermo Fisher) for 20 min at RT in the dark. After, cells were centrifuged at 2,600 rpm for 5 min, washed with staining buffer and stained in a volume of 50  $\mu$ L/well with anti-CD56-FITC (B159; Becton Dickinson), anti-CD3-PE-Cy7 (SK7, Becton Dickinson), anti-CD4-AF700 (RPA-T4, Becton Dickinson), anti-E-cadherin-PE-CF594 (67A4, Becton Dickinson), and anti-KLRG1-BV421 (14C2A07, Biolegend), for 20 min at RT. After the cell surface staining, cells were washed with staining buffer, fixed and permeabilized with Fixation/Permeabilization Solution (Becton Dickinson) for 20 min at 4°C, washed with BD Perm/Wash buffer, and stained with anti-p24-PE (KC57-RD1, Beckman Coulter) for 20 min on ice and 20 min at RT. Finally, cells were washed and fixed with 2% PFA. Samples were acquired in an LSR Fortessa flow cytometer (Becton Dickinson) and analyzed using FlowJo V10 software. We calculated target cell killing as the reduction in infected (p24<sup>+</sup>) cells. In some experiments, we studied the impact on the NK cytotoxic function of blocking the E-cadherin in the cell targets. In such cases, HIV-infected CD4<sup>+</sup> T cells were previously treated with an E-cadherin neutralizing antibody (clone DECMA-1, Biolegend) or the isotype control rat IgG1 k

(RTK2071, Biolegend) for 20 min and then washed with staining buffer to remove the unbound antibodies before the co-culture with NK cells. The natural cytotoxicity assay was performed as described above.

### FACS isolation of KLRG1<sup>+</sup> NK cells and CD4<sup>+</sup> T cells

For Fluorescence-Activated Cell Sorting (FACS), 100 million PBMCs from ART-suppressed PWH were stained with LIVE/DEAD Far Red viability (Invitrogen) for 20 min at RT. After washing with 1X PBS, cells were surface stained with anti-CD56-FITC (B159, Becton Dickinson), anti-CD3-PE-Cy7 (SK7, Becton Dickinson), anti-CD19-APC-Fire750 (HIB19, Biolegend), anti-CD16-BV786 (3G8, Becton Dickinson), anti-CD4-BV605 (RPA-T4, Becton Dickinson), anti-CD8-V500 (RPA-T8, Becton Dickinson), and anti-KLRG1-BV421 (14C2A07, Biolegend) antibodies for 20 min at RT. Cells were then washed with staining buffer and immediately sorted using the Cytex Aurora Cell Sorter. We sorted the live populations CD4<sup>-</sup>CD3<sup>-</sup>CD56<sup>+</sup>KLRG1<sup>+</sup> (KLRG1<sup>+</sup> NK cells), CD4<sup>-</sup>CD3<sup>-</sup>CD56<sup>+</sup>KLRG1<sup>-</sup> (KLRG1<sup>-</sup> NK cells), CD3<sup>+</sup>CD4<sup>+</sup>CD56<sup>-</sup>KLRG1<sup>+</sup> (KLRG1<sup>+</sup> CD4<sup>+</sup> T cells) and CD3<sup>+</sup>CD4<sup>+</sup>CD56<sup>-</sup>KLRG1<sup>-</sup> (KLRG1<sup>-</sup> CD4<sup>+</sup> T cells). The purity of the cells was >95% in all cases.

### Viral reactivation in ART-suppressed PWH samples

CD4<sup>+</sup> T cells from ART-suppressed PWH were isolated using a commercial kit (MagneSort Human CD4<sup>+</sup> T cell Enrichment; Affymetrix) and cultured in R10 medium with Q-VD-OPH (Selleckchem) for 2 h in the presence of Raltegravir (1 μM), Darunavir (1 μM), and Nevirapine (1 μM) to prevent new rounds of viral infection. After 2 h, PMA (Abcam) plus ionomycin (Abcam) (PMA 81 nM; ionomycin 1 μM) were added to the cell culture as a latency reversal agent and left for 18 h to reactivate latent HIV. After viral reactivation, cells were subjected to natural cytotoxicity assays as described above. After, cells were stained with LIVE/DEAD Far Red viability for 20 min at RT and then with anti-CD56<sup>-</sup> FITC (B159; Becton Dickinson), and anti-CD3-PerCP (SK7, Becton Dickinson) antibodies for 20 min at RT. After the cell surface staining, cells were fixed and permeabilized with Fixation/Permeabilization Solution (Becton Dickinson) for 20 min at 4°C, washed with BD Perm/Wash buffer, and stained with anti-p24-PE (Beckman Coulter) for 20 min on ice and 20 min at RT. Finally, cells were washed and fixed with 2% PFA. Samples were acquired in a FACSCalibur flow cytometer (Becton Dickinson) and analyzed with FlowJo V10 software. The limit of detection of our assay is established at 50 p24<sup>+</sup> cells/million CD4<sup>+</sup> T cells as previously reported.<sup>40</sup>

### NK killing of cells harboring intact provirus

CD4<sup>+</sup> T cells from ART-suppressed PWH were isolated using the Dynabeads CD4 Positive Isolation Kit (Affymetrix) and cultured in R10 medium at a concentration of 1.5 M/mL in the presence of an ART cocktail (Raltegravir, Darunavir, and Nevirapine at 1 μM each) to prevent new rounds of viral infection. To reactivate latent HIV, PMA (81 nM) and Ionomycin (1 μM) were added to the cell culture as a latency reversal agent, and the cells were left for 18 h. The negative fraction of cells remaining from the CD4<sup>+</sup> T cell isolation kit were cultured overnight in R10 medium supplemented with 100 U/mL of IL-2 (Merck) at a concentration of 2 M/mL. The following day, NK cells were enriched from the CD4<sup>-</sup> fraction using the MagneSort Human NK cell Enrichment Kit (Invitrogen). After viral reactivation, a natural cytotoxicity assay was conducted, wherein NK cells were seeded in a 96-well round-bottom plate and cocultured with reactivated CD4<sup>+</sup> T cells at a 1:1 ratio in R10 medium containing the ART cocktail plus DNase (100 μg/mL, Merck). Enriched NK cells were pre-incubated with either IgG2a isotype control at 10 μg/mL (MOPC-173, Biolegend) or human purified anti-KLRG1 at 10 μg/mL (14C2A07, Biolegend) for 20 min, followed by a single wash with PBS 1X. After 4 h of incubation at 37°C in 5% CO<sub>2</sub>, the remaining viable CD4<sup>+</sup> T cells were isolated from the coculture using a combination of the EasySep Dead Cell Removal (Annexin V) Kit (StemCell Technologies) and the MagneSort Human CD4<sup>+</sup> T cell Enrichment Kit (Invitrogen). The cell pellet was then lysed with proteinase K-containing lysis buffer and incubated at 55°C overnight, followed by a 95°C incubation for 5 min, to obtain DNA for the Intact Proviral DNA Assay (IPDA) described below.

### Intact proviral DNA assay (IPDA)

IPDA was performed as described before<sup>62</sup> and using primers and probes specific for the  $\Psi$  HIV gene (HIV-1  $\Psi$  forward 5'-CAG GACTCGGCTTGCTGAAG-3', HIV-1  $\Psi$  reverse GCACCCATCTCTCCTTCTAGC and probe 5' 6-FAM-TTTTGGCGTACTCAC CAGT-MGBNFQ-3') and *env* HIV gene (HIV-1 *env* forward 5'-AGTGGTGCAGAGAGAAAAAAGAGC-3', HIV-1 *env* reverse 5'-GTCTGGCCTGTACCGTCAGC-3', HIV-1 *env* intact probe 5'-VIC-CCTTGGGTTCTTGGGA-MGBNFQ-3', and HIV-1 anti-Hypermutant *env* probe 5'-CCTTAGGTTCTTAGGAGC-MGBNFQ-3'). The hRPP30 gene was used for cell input normalization. Samples were analyzed in a QIAcuity One 2-plex System (Qiagen).

### Quantification of HIV DNA and RNA by qPCR

CD4<sup>+</sup> T lymphocytes were enriched from total PBMCs using a negative selection kit (MagneSort Human CD4<sup>+</sup> T cell Enrichment, eBioscience) or isolated by FACS. Then, CD4<sup>+</sup> T cells were used for both HIV DNA and RNA quantification. CD4<sup>+</sup> T cells for HIV-DNA analysis were immediately lysed with proteinase K-containing lysis buffer (at 55°C overnight and 95°C for 5 min). The HIV DNA in the cell lysates was quantified by quantitative PCR (qPCR) using primers and probes specific for the 1-LTR HIV region (LTR forward 5'-TTAAGCCTCAATAAAGCTTGCC-3', LTR reverse 5'-GTTCCGGGCGCCACTGCTAG-3' and probe 5'/56-FAM/CCAGAGTCA/ZEN/CACAACAGACGGGCA/31ABkFQ/3'). The CCR5 gene was used for cell input normalization. Samples were analyzed in an Applied Biosystems 7000 Real-Time PCR System. For Viral RNA quantification, CD4<sup>+</sup> T cells were subjected to RNA extraction using the

RNeasy plus micro (Qiagen) kit (for less than 0.5M cells) or NZY Total RNA kit (NZYtech) (for a number of cells ranging between 0.5 and 5M) following the manufacturer's instructions. Reverse transcription of RNA to cDNA was performed with the SuperScriptIII (Invitrogen), and cDNA was quantified by qPCR with primers against the HIV long terminal repeat (LTR). Quantification of RNA and DNA copies was performed using a standard curve, and values were normalized to 1 million CD4<sup>+</sup> T cells. For testing the effect of the anti-KLRG1 antibody in CD4<sup>+</sup> T cells from ART-suppressed PWH, CD4<sup>+</sup> T cells were isolated by magnetic beads as described here and cultured in R10 medium with Q-VD-Oph (Selleckchem) for 2 h in the presence of Raltegravir (1 μM), Darunavir (1 μM), and Nevirapine (1 μM). After, cells (at least 1 M per condition) were incubated with the anti-KLRG1 antibody (6 μg/mL) or an IgG2a isotype (6 μg/mL). Cells incubated with romidepsin (40 nM) were included as a positive control. Cells were cultured for 20 h and after, viral reactivation was quantified by the intracellular detection of HIV-RNA, as described above.

### QUANTIFICATION AND STATISTICAL ANALYSIS

Statistical analyses were performed with Prism software, version 6.0 (GraphPad). A p value < 0.05 was considered significant. Volcano plots were automatically produced by the OMIQ software, and differences were regarded as statistically significant when the value of p or the False Discovery Rate (FDR) value were below 0.05. The statistical details for the different experiments can be found in each figure legend.